UNIVERSITAT ROVIRA i VIRGILI

DISTRICT HEATING DRIVEN ABSORPTION HEAT PUMP FOR SPACE HEATING AND COOLING APPLICATIONS IN NON-RESIDENTIAL BUILDINGS

MUHAMMAD FAIQ VIDI WARDHANA

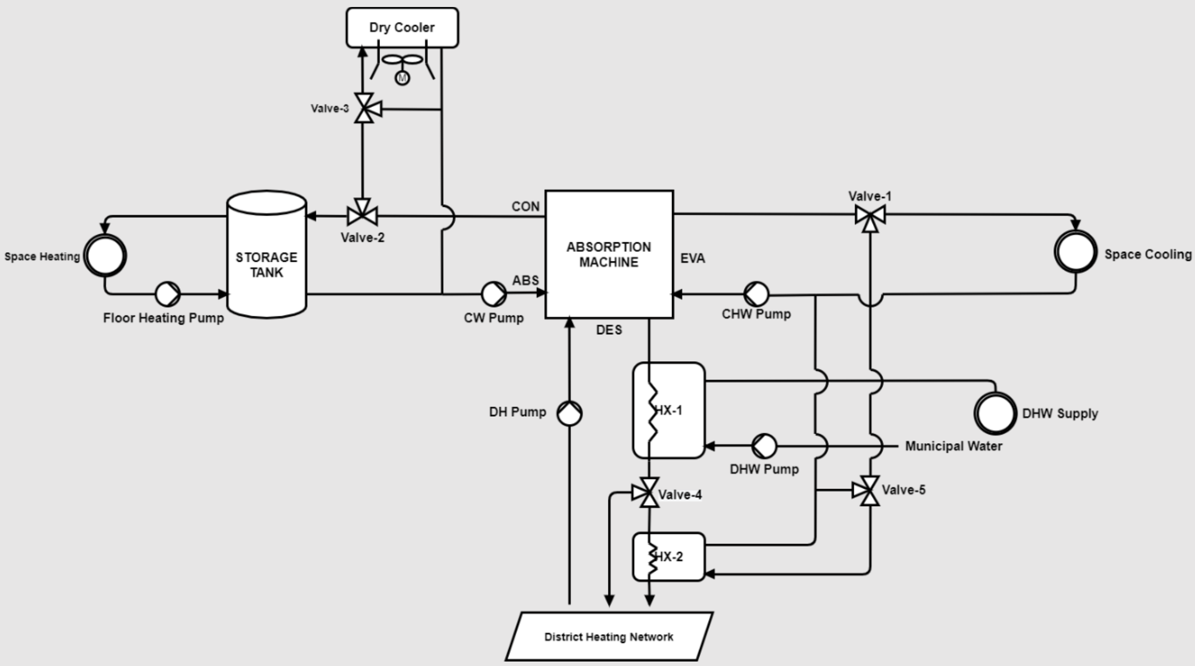

MASTER THESIS

2021

Muhammad Faiq Vidi Wardhana

District Heating Driven Absorption Heat Pump for Space Heating and Cooling Applications in Non-Residential Buildings

MASTER'S THESIS

Supervised by

Dr. Dereje Sendeku Ayou

Prof. Dr. Alberto Coronas Salcedo

Master's Degree

in Energy Conversion Systems and Technologies

UNIVERSITAT ROVIRA i VIRGILI

Tarragona, February 2021

UNIVERSITAT
ROVIRA I VIRGILI
DEPARTAMENT D'ENGINYERIA MECÀNICA
Escola Tècnica Superior d'Enginyeria Química (ETSEQ).
Avgda Paisos Catalans, 26 ; 43007 Tarragona (Spain)

DECLARATION

We STATE that the present master thesis, entitled "District Heating driven Absorption Heat Pump for Space Heating and Cooling Applications in Non-Residential Buildings" presented by Muhammad Faiq Vidi Wardhana, has been carried out under our supervision at CREVER Research Group in the Department of Mechanical Engineering of Rovira i Virgili University.

Tarragona, February 10, 2021

Dereje S. Ayou

Alberto Coronas

ACKNOWLEDGEMENTS

First of all, I want to express my deepest gratitude to The Almighty God, Allah S.W.T, for His blessings and grace so I can complete this master thesis right on time. I also thank Him for the health and all the benefit that I had during the process of this master thesis.

Secondly, this acknowledgment belongs to my beloved mom Evi Despriyanti who always pray for his son to be the better person through this master's program, my girlfriend Cut Safira Zulva who always be there for me during my darkest time, and to my sister Annisa Ayu Wardhani who supports me unconditionally.

Surely, I would like to give my highest appreciation to Dr. Dereje Sendeku Ayou and Prof. Alberto Coronas for all their support and availability during this work. I am very much thankful for their guidance, encouragements, and advices. I also want to extend my highest recognition to all other professors that have helped me throughout this master's degree program.

Last but not least, I want to say thank you to all my friends that have entertained and made me happy during this study, especially to Habibie Muhammad Ega and Reza Harigyanto as my flat mates and partners in this journey.

ABSTRACT

Over the last decade, significant progress has been made in the development of absorption heat pump/chiller technologies with useful characteristics for reversible operation in heating and/or cooling mode and connection to district heating network because of large temperature gliding in the driving heat source stream. The main motive to drive such type of absorption heat pumps with district heating networks include extended annual operation hours for both the absorption machine and district heating network. This master thesis describes the performance of absorption machine connected to the district heating network in different locations representing different operating conditions that operate in heating and cooling mode for non-residential buildings. The results are obtained from the annual performance simulation using TRNSYS software by defining the absorption machine behaviour using its characteristic equation in EES software. The analysed results are seasonal COP of the absorption machine in heating and cooling mode as well as the potential domestic hot water produced. Further in this work, the annual operation hour and the primary energy ratio of the proposed system are presented. The primary energy ratio then is compared with a typical conventional cooling and heating system. It is found that the proposed system consumes less primary energy. Thus, the development of this type of system contributes towards the reduction of fossil fuel consumption for the space cooling and heating sector of non-residential buildings.

Keywords: Absorption heat pump, District heating, Performance simulation, Reversible operation, Degree-Days.

LIST OF ABBREVIATIONS

General:

ABS	Absorber
ACH	Air Changes per Hour
ASHRAE	The American Society of Heating, Refrigerating, and Air-Conditioning Engineers
Cfm	Cubic Foot per Minute
CHP	Combined Heat and Power
CHW	Chilled Water
CIBSE	The Chartered Institution of Building Services Engineers
CON	Condenser
CW	Cooling Water
DD	Degree-Days
DES	Desorber
DH	District Heating
DHW	Domestic Hot Water
EES	Engineering Equation Solver
EVA	Evaporator
HX	Heat Exchanger
IWEC	The International Weather for Energy Calculation
TRNSYS	Transient System Simulation Software

Variables:

COP	Coefficient of Performance (-)
GFR	Glass to Frame Ratio (-)
HLC	Building Heat Loss Coefficient (kW/K)
PE	Primary Energy (kW)
PER	Primary Energy Ratio (-)
PES	Primary Energy Savings (kW)
$\dot{Q}$	Thermal Power (kW)
Q	Thermal Energy (kWh)
R	Thermal Resistance (m^2K/W)

SHGC	Solar Heat Gain Coefficient (-)
T	Absolute Temperature (K)
t	Temperature (°C)
U	Thermal Transmittance (kW/m^2K)

Subscript:

AC	absorber - condenser
Ai	absorber inlet
amb	ambient condition
b	base
C	cooling mode
c	cold side of heat exchanger
Co	condenser outlet
D	desorber
db	dry bulb
dh	district heating
Di	desorber inlet
Do	desorber outlet
E	evaporator
Ei	evaporator inlet
el	electricity
Eo	evaporator outlet
G	gain
H	heating mode
h	hot side of heat exchanger
in	indoor
prim	primary energy
ref	reference
se	external surface
si	internal surface
th	thermal
VCC	vapor compression chiller

LIST OF FIGURES

LIST OF TABLES

CONTENTS

1. INTRODUCTION

1.1 Background

Over the years, energy sources and primary energy utilization have been an issue around the world. From the primary energy point of view, the issue is that fossil fuel is still widely used to provide the energy demand in all sectors. As it can be seen in Figure 1.1, the consumption of petroleum products in Europe accounts for 39.6% (Bertoldi P *et al.*, 2018), which is the highest energy consumption among other fuel types. Fossil fuel is non-renewable energy that leads to the energy crisis due to the limitation of fossil fuel availability (Li *et al.*, 2011). Moreover, the issue is not only to the availability of the fuel, but also the adverse impact of fossil fuel utilization on the environment. Studies reported that the earth will have a higher temperature as long as the fossil fuel is used continuously (Zecca and Chiari, 2010). Due to all these factors, it is very reasonable that the campaign to stop the use of fossil fuel is now being a movement. A lot of investigations have been developed to find a way of how to reduce and even substitute fossil fuels (Li *et al.*, 2011). Among all the new systems, district heating is proven to be able to reduce the use of fossil fuel and even eliminate it. This is because the energy source to generate heating can be obtained from various types of fuel. Moreover, it has a very good prospect for being part of the future energy transition (Sorknæs *et al.*, 2020).

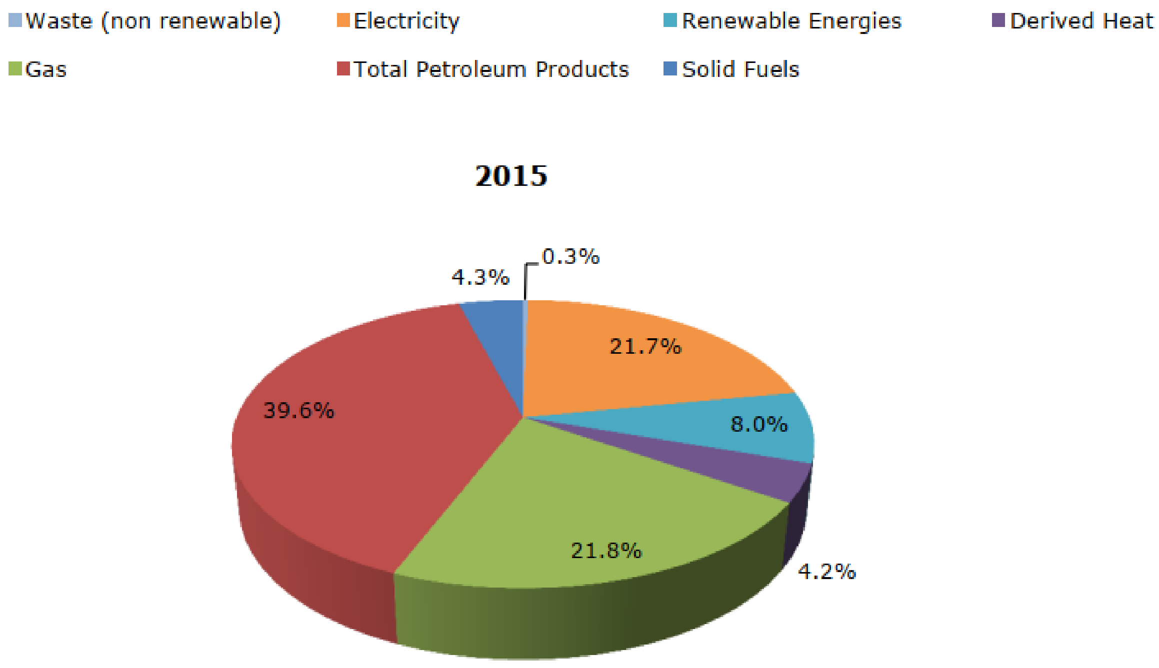

Figure 1.1. Final energy consumption based on fuel type in Europe 2015 (Bertoldi P *et al.*, 2018)

According to the American Society of Heating, Refrigerating, and Air-Conditioning Engineers (ASHRAE) (Phetteplace *et al.*, 2013), district heating is a system that distributes thermal energy in the form of hot water or steam from a thermal generation plant to the end-users to support their energy demand. From this definition, it can be said that the district heating is like the electricity grid but in a different form of energy. District heating can be obtained by utilizing the waste heat from the power generation plant, such as in CHP (Lund *et al.*, 2010). Thus, the efficiency of the plant will increase, and it will reduce the combustion of fossil fuels. District heating can also be obtained from industrial waste heat, moreover, it can be obtained from renewable energy such as biomass or even solar thermal (Werner, 2017). District heating has a flexible combination with electricity such as the integration with CHP Plant, electric boilers, and heat pumps (Sorknæs *et al.*, 2020). In the industrial sector, district heating is used mainly for process heating and humidification. While for the residential and commercial buildings, the typical use of district heating is to cover the energy demand for domestic hot water supply, cooking, space heating, and even for space cooling through thermally driven chiller (Phetteplace *et al.*, 2013).

The use of district heating to cover the demand for space heating and cooling seems to be an interesting application since 50% of the total final energy demand is coming from the space heating and cooling in buildings (Bertoldi P *et al.*, 2018). Moreover, energy consumption from cooling and heating demands is increasing around the world (Kühn *et al.*, 2010). This phenomenon occurs due to several factors such as the growth of the population and change of lifestyle. Another factor that should be pointed out is the increase of earth temperature as the environmental impact from the use of non-renewable energy (Chardon *et al.*, 2020). One of the technologies that can be applied to extract the energy from the district heating network to cover the space cooling and heating demands is by the application of an absorption heat pump.

According to Herold et al. (2016), "heat pump" is technology that transfers heat from a low-temperature source to a high-temperature sink. Heat pumps can be classified based on the type of driving energy: work-driven heat pump and heat-driven heat pump. From its classification, it can be seen that the heat pump requires either work or heat as a driving energy input. In the field of space heating and cooling applications, the work-driven heat pump is a vapor compression cycle device while one of the heat-driven heat pumps is an absorption cycle device. Thus, it is clear that the definition of an absorption heat pump is a technology based on the absorption refrigeration cycle that uses heat as the driving heat to provide heating or cooling demand. The difference between the basic absorption heat pump and vapor-compression heat pump cycles can be seen in Figure 1.2.

As it can be seen in Figure 1.2, the absorption heat pump has four main components that exchange heat with its surroundings (heat source and heat sink streams), which are absorber, condenser, evaporator, and desorber (generator). The evaporator operates at a low temperature and pressure level. It has a function to transfer the heat from the source to the refrigerant, while the absorber and condenser operate at the intermediate temperature level where they reject the heat to the sink. Desorber operates at the highest temperature level. It has a function to take the heat from the driving heat source into the system. In the case of vapor compression heat pump, the driving energy (i.e. work input) is supplied to the compressor. The work supplied for the vapor-compression heat pump comes from the electricity, while the driving heat for absorption heat pump can be obtained from any available heat source at a suitable temperature level such as a solar thermal, geothermal, direct couple with cogeneration plant, even district heating network.

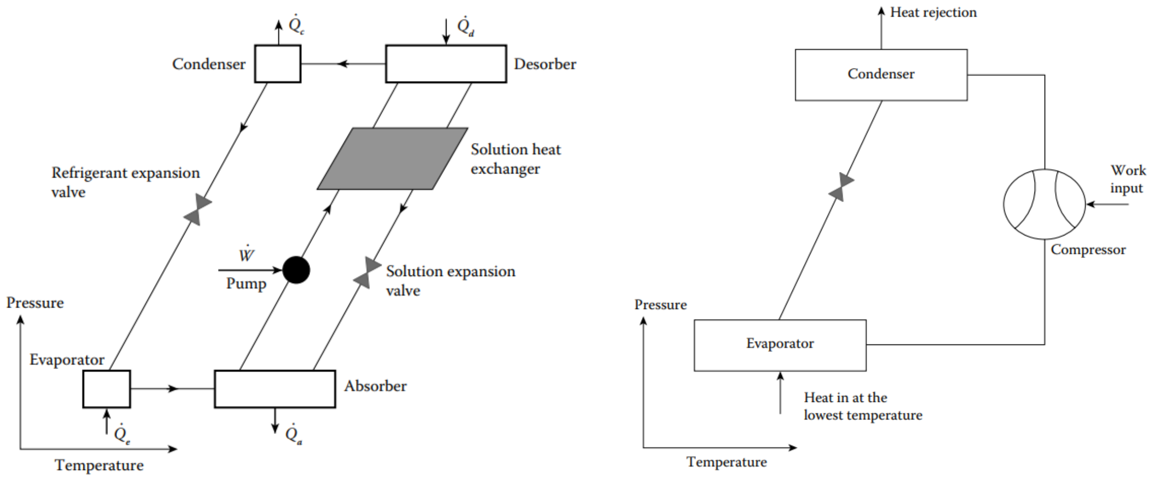

Figure 1.2. Left: single-effect absorption heat pump; Right: vapor-compression heat pump. (Herold, Radermacher and Klein, 2016)

Although the vapor-compression chillers and heat pumps are more common in the market due to their wide range of type and simplicity, the use of absorption heat pump should be considered because it can reduces electricity demand (Ayou and Coronas, 2020), which is favourable because consequently it will also save the electricity cost and reduce the utilization of fossil fuel when it is coupled with heat generated from environmentally friendly energy such as solar thermal or district heating from non-fossil fuel.

The district heating network-driven absorption heat pump can produce cooling and heating by using heat from a district heating network through the reversible operation. For non-residential building in four-season countries, this application can be used to provide space cooling during the hot season and space heating during the cold season. Moreover, it can also produce domestic hot water to cover the available demand of the end-user. Hence, the application of the absorption heat pump in reversible operation is beneficial throughout the year (Chardon *et al.*, 2020), as a result, it will provide an economic benefit to the user.

Figure 1.3. A newly developed 50 kW absorption chiller from Baelz manufacturer

(Baelz Automatic, 2020b)

The Technical University of Berlin has designed and developed a new generation of an absorption heat pump in collaboration with ZAE Bayern and Vattenfall Europe (Petersen *et al.*, 2013). In 2010, they investigated a 10 kW (in cooling mode) absorption heat pump with the reversible operation in different possible heat sources and heat sinks (Kühn *et al.*, 2010). In the following years, they carried out experimental studies and published the performance of their 50 kW absorption chiller along with its integration into the district heating network (Petersen *et al.*, 2011). After several years of doing the development and field tests, the commercial product was released as shown in Figure 1.3. Their product consists of three different nominal cooling capacities: 50 kW, 160 kW, and 500 kW (Baelz Automatic, 2020a). Ayou and Coronas (2020) reported that this product has a high energy efficiency in cooling mode (thermal cooling COP > 0.75), lower minimum driving heat temperature (< 60°C), high rejection temperature (> 45°C), and large glide temperature in the driving heat source stream (18 K).

1.2 Justification

From the background of this master thesis, it is said that the new hot water driven efficient and compact absorption heat pump has shown some advantages. Of course, this machine has passed a lot of laboratory and field tests before commercialization. However, it's the annual performance to cover space cooling and heating demands while operating in reversible mode has not been investigated. It is necessary to see the annual performance of this absorption machine to determine its capability in space cooling and heating applications. In the manufacturer's catalogue (Baelz Automatic, 2019), it is stated that the machine can be operated in a reversible mode as a chiller and heat pump. However, the performance of this machine available in the literature was limited to cooling mode as an absorption chiller (Petersen *et al.*, 2011, 2013; Albers and Ziegler, 2016; Hüls Güido *et al.*, 2018). Therefore, it is interesting to investigate the performance of this machine in reversible operation throughout the year; thereby, it's the energetic advantages can be evaluated. Also, the machine's annual operational characteristics when coupled with district heating network can be better understand. The development of this type of system (i.e. reversible absorption heat pump coupled to district heating network) contributes towards the reduction of fossil fuel consumption in the space cooling and heating sectors of non-residential buildings (e.g. office buildings).

This master thesis includes the knowledge of subject Characterization and Modelling of Energy Demand in Buildings (Carrillo, 2020) in the estimation of space heating and cooling demand using degree-days method, Thermal Conversion Energy Technologies (Coronas, 2020) in the utilization of absorption machine to cover the space cooling and heating demands, Modelling and Dynamic Simulation of Energy Conversion Systems (Prieto, 2020) in the system simulation, and Polygeneration of Energy and Energy Integration (Bruno, 2020) as the desired output for system comparison.

1.3 Objective

The study of integrating reversible absorption heat pump with the district heating network to supply thermal energy demands (i.e. cooling, heating, and domestic hot water) in a non-residential building will be carried out. The goal is to evaluate the performance of the proposed system through numerical modelling and simulation. Additionally, the annual energy performance for the provision of space cooling in summer and space heating in winter (as well as domestic hot water supply throughout the year) will also be investigated. The main tasks also included in this study is the estimation of space cooling and heating demands in different ambient conditions representing different geographical locations. Finally, the performance comparison between the proposed system configuration (absorption heat pump driven by district heating network) with the conventional heating and cooling systems in the non-residential sector will be discussed.

1.4 Scope and Limitation

The scope of this master thesis as well as the limitations are:

- Space cooling and heating demand estimation for the non-residential building is using the method of degree-days with variable based temperature. The method only takes into account the sensible heat.
- The building reference used in the calculation is a typical office building reference released by the Department of Energy USA in 2011 (US Department of Energy, 2012).
- The absorption machine is modelled based on the published characteristic equation of the newly developed efficient and compact water/LiBr absorption heat pump of 50 kW (in cooling mode) (Albers and Ziegler, 2016) with a constant mass flow rate for all the external circuits.
- The constant inlet desorber hot water temperature is represented based on the design district heating temperature in selected locations.
- TRNSYS is used as a simulation tool (TRNSYS16, 2007).

1.5 Thesis Structure

In this master thesis, there are five chapters. Chapter 1 details the problem, objectives, and scope of the research. Chapter 2 shows an overview of the state of the art about district heating networks, the absorption chiller used in the present study, and the space cooling and heating demand estimation. This chapter also includes the data of design district heating supply temperature in some European Countries, the behaviour of the considered absorption chiller in both cooling and heating modes based on its characteristic equation, and the description of the applied degree days method. Chapter 3 shows the methodology of how this master thesis research is carried out. It includes the selected case study for space cooling and heating demand calculation as well as the assumption used for the simulation. Chapter 4 is intended to show the result of this research. The analysis and explanation are also carried out in this chapter. Finally, chapter 5 shows the conclusions of the research.

2. APPROACH

This chapter contains the conceptual development of the methodology of this master thesis. It explains about the state of the art of district heating technologies, the water/LiBr absorption heat pump in reversible operation, and space cooling and heating demands estimation based on degree-days method.

2.1 District Heating Systems

Similar to the definition from ASHRAE in the introduction, district heating is defined as a heating system that transmits and distributes heat from one or more energy sources to residential, commercial, and industrial customers for space heating or hot water heating (Li *et al.*, 2011). From this definition, it is understandable that instead of generating heat on-site or in each facility, the heating effect comes from a distribution medium (Phetteplace *et al.*, 2013). The fundamental objective of the district heating is to use the local fuel or heat sources that would otherwise be wasted in order to cover customer heating demand efficiently by using a heat distribution pipe network as a local market place (Werner, 2013). As it is mentioned in chapter 1, there is a lot of possibility of energy sources to generate this system, from fossil fuel combined heat and power plants to waste-to-energy plants, geothermal plants, solar collectors, biomass energy, etc. Nowadays, the utilization of renewable energy to produced useful heat is the major challenge for district heating networks around the world (Martin, 2019).

2.1.1 Description

District heating network has three primary subsystems (Figure 2.1) (Sayegh *et al.*, 2018):

- Thermal energy production subsystem

  This subsystem has a purpose to produce the thermal energy needed to increase the temperature from the return line of the district heating network until the temperature reaches the desired supply temperature. There are multiple options according to the primary energy source of which the thermal energy production subsystem can be applied. It could be from CHP Plant, geothermal plant, household waste heating plant, biomass heating plant, etc. However, the utilization of CHP Plants as the thermal energy production subsystem for district heating network has been the strongest candidate among other systems (Werner, 2017). It is because the unavoidable heat losses from thermal power plants can be recuperated for other heat purposes. The thermal energy production subsystem is represented by the central heating plant in Figure 2.1.

- Thermal energy transport subsystem

  This subsystem has two purposes. It distributes the thermal energy that has been produced by the thermal energy production subsystem to the consumer in the form of steam or hot water. The other purpose is to return the steam or hot water from the consumer to the thermal energy production subsystem. The return line has a lower temperature since the energy produced is used by the consumer.

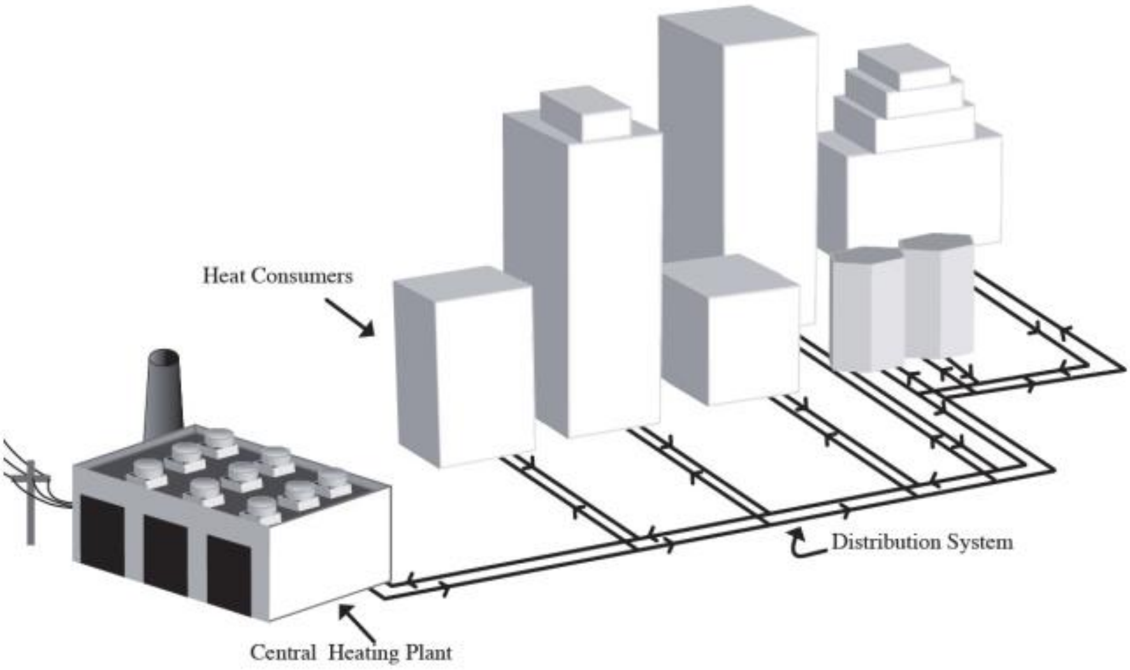

Figure 2.1. Basic system of district heating network (Phetteplace *et al.*, 2013)

- Consumer interconnection (direct or indirect)

  Each consumer has their interconnection to extract the energy from the primary district heating network according to the type of demand. Direct interconnection means that the consumer is using the primary network directly to obtain the demand, while indirect interconnection means that the consumer is using a secondary network. The secondary network is used to cover the demand for domestic hot water, space heating, and space cooling (using a thermally driven cooling device) of the building (Chardon *et al.*, 2020). The primary and secondary networks are connected via a heat exchanger to cover the demand for space heating and domestic hot water (Euroheat & Power, 2008). However, in order to increase the efficiency of the district heating system, recent studies suggest that absorption heat pumps can be used to cover the demand of space heating, even also space cooling (Werner, 2017).

2.1.2 Evolution of District Heating Network

As it can be seen in Figure 2.2, the first generation of district heating network was built in the 1880s. The system was using steam to distribute the thermal energy. The energy transport subsystem is steam pipes in concrete ducts. The pressure could be as high as 25 bars and the temperature equal to 180°C (Martin, 2019). The second-generation technology appeared in the 1930s until the 1980s and it was using a pressurized hot water system. The third-generation technology, which is still used today, was developed in the 1970s and 1980s when buildings had high heat demands and heat production was based on fossil fuel. The system uses hot water with temperatures below 100°C using pre-insulated pipes. From this explanation, it can be said that the development of the district heating network was based on the idea to decrease the supply temperature in order to increase the energy efficiency as well as minimizing the heat losses (Çomakli *et al.*, 2004). The fourth generation is using water temperature around or even below 65°C, allowing more contribution of renewable energy and geothermal plants as the thermal energy production subsystem.

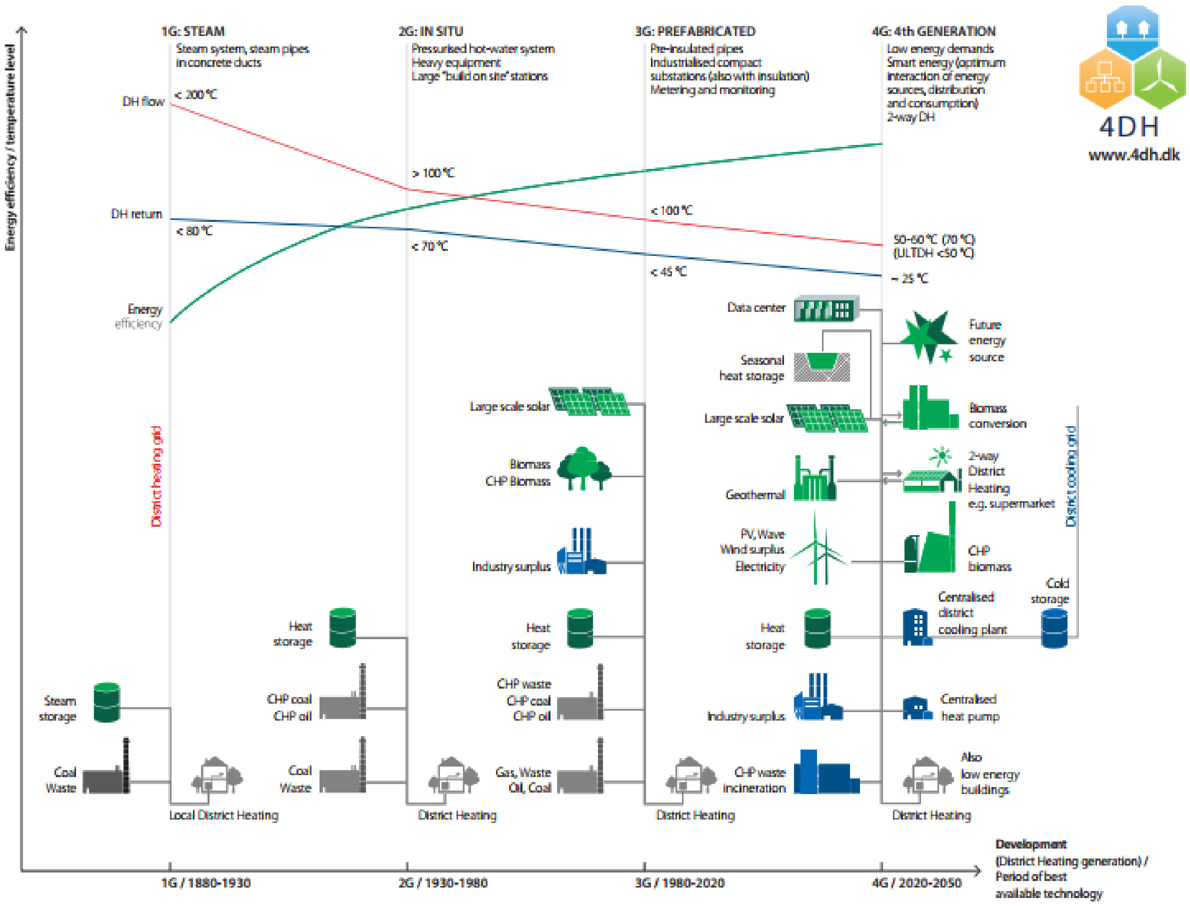

Figure 2.2. Evolution of district heating network (Thorsen *et al.*, 2018)

2.1.3 District Heating Network in The World and Europe

District heating now can be found almost in every part of the world. The number of installed district heating is expected to reach 80,000 networks where 6000 of them are located in Europe (Werner, 2013). As it can be seen in Figure 2.3, the main users of district heating are Russia, China, and European Union, with 85% of the total energy deliveries. This data does not take into account the district heating network operated by the consumer itself such as military group which is the common case in the USA (Werner, 2017).

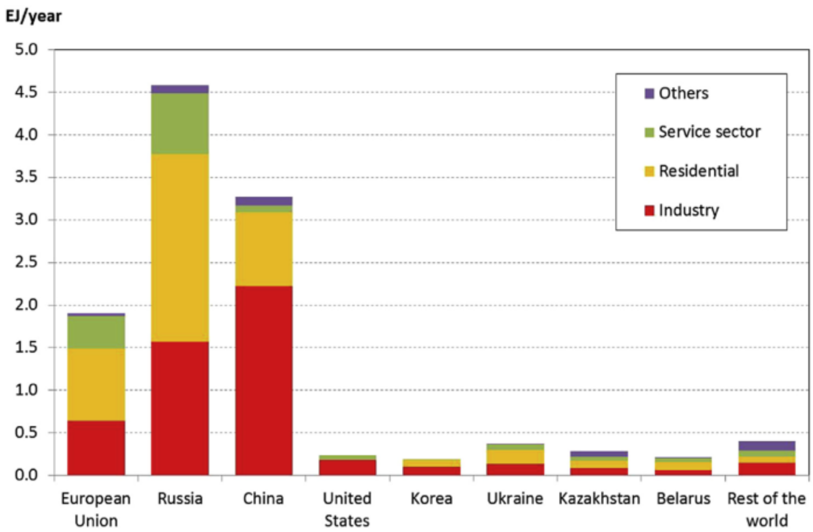

Figure 2.3. Heat deliveries in various regions and countries during 2014 according to different users (Werner, 2017)

In the case of energy production subsystem type, European Union uses mainly from CHP plants which account for the proportion of 72%, while the rest of 27% comes from renewable heat systems. In comparison to the world, the proportion of heat produced by CHP plants is 59% and 9% from renewable energy sources. This lower statistic is influenced by Russia and China that only use 50% of CHP plants as their energy production subsystem (Werner, 2017), and the other 50% is contributed by China's commitment to the direct use of coal and Russia to natural gas in heat-only boilers (Martin, 2019).

2.1.4 Design Supply Temperature of District Heating in Europe

In Europe, the operating temperature of district heating system varies according to the national regulations and design guidelines (Mora *et al.*, 2017). An overview of some national design supply temperature is shown in Table 2.1. The return temperature refers to the maximum allowed temperature (Euroheat & Power, 2008). In other word, ideally, the return temperature cannot be higher than these temperatures. However, more efficient district heating is desirable by reducing the supply temperature (for example: from the third generation to the fourth generation of district heating network) or increasing the temperature difference between supply and return temperature (Skagestad and Mildenstein, 2002).

Table 2.1. National design temperature for district heating (Skagestad and Mildenstein,2002)

Country	Supply Temperature (°C)	Return Temperature (°C)
Denmark	70	40
Finland	70	40
Korea	70	50
Romania	95	75
Russia	95	75
United Kingdom	82	70
Poland	85	71
Germany	80	60

In Spain itself, ENGIE, a French energy company, in partnership with Tersa, Aigüas de Barcelona, Instituto para la Diversificación y Ahorro de la Energía (IDAE), and Institut Català d'Energia (ICAEN), set up the first district heating network of the country called Districlima in 2004 (Districlima, 2014). As of December 2018, the customer of this district heating network has reached over 100 large buildings in Barcelona, reducing 73% of fossil fuel consumption in space heating and cooling (Districlima, 2019). The district heating network line of Districlima can be seen in Figure 2.4. According to the technical specification of Districlima (2020), the supply temperature of hot water is 90°C while the maximum return temperature is 60°C.

Figure 2.4. District heating network line of Districlima in Barcelona 2018 (Districlima, 2019)

2.2 Absorption Machine Technologies

As it is introduced briefly in the introduction of the master's thesis, absorption heat pump is a technology based on absorption cycle that requires heat as the energy input. The difference from the conventional heat pump is that the conventional vapor compression heat pump uses energy input in the form of electricity. Therefore, this technology is suitable to couple with district heating as the driving heat and contributes to electricity savings. According to Herold et al. (2016), a common product of absorption technologies in the market consists of several type of systems, such as single-effect, double-effect and triple-effect water/lithium bromide absorption chillers and heat pumps. Also, there are ammonia/water heat pumps and refrigerators in the market for residential and industrial applications, respectively.

As it is explained above, the current market is commonly used water/lithium bromide and ammonia/water as the working fluid mixture of the system. However, other working fluids that are under development or already in the market with a miner market share (Chardon *et al.*, 2020). The overall working fluids for absorption machine in the market can be seen in ASHRAE Fundamental Handbook directly (ASHRAE, 2017). In the following section, a single-effect water/lithium bromide absorption heat pump will be described.

2.2.1 Single-effect Water/Lithium Bromide Absorption Heat Pump

There are four main components in the single-effect water/lithium bromide absorption heat pump: the evaporator, absorber, desorber, and condenser. The main processes involved are (Hundy *et al.*, 2016):

1. The refrigerant evaporates in the evaporator, by extracting heat from the low-temperature heat source (external circuit of evaporator: chilled water).
2. The vapour from the evaporator that contains heat from a low-temperature level flows to the absorber and mixes with the solution of a strong concentration of lithium bromide that flows from the desorber. The mixing process will release some heat, in this case, the heat is transferred to the medium temperature level by the external circuit of the absorber.
3. The mixture of vapour and the strong solution is called the weak solution. This solution is pumped to the desorber. The pump increases the pressure of the solution. In the desorber, the weak solution receives heat from the driving heat, increasing the temperature of the weak solution that turns into a desorption process: generation of water vapour from weak solution. In consequence, the concentration of absorbent

increases, and thus the solution becomes the strong solution in lithium bromide. The vaporized water is the refrigerant of the system.

4. The refrigerant vapour goes to the condenser and releases heat. The heat then is rejected to the medium temperature level by the external circuit of the condenser. Thus, the phase of the refrigerant now is saturated liquid or even subcooled.
5. The refrigerant's pressure leaving the condenser is then reduced by an expansion valve before entering the evaporator again. This expansion process yields to the phase change of the refrigerant as well as the significant temperature drop of the refrigerant. Then, this cyclic process repeats step 1.

As it is explained, the main components are in charge of the heat transfer process, there is no work interaction in the main components. The work is only in the solution pump, which contributes to a very small portion of the system's energy consumption. There are three types of connection between the external circuit of the condenser and absorber. The parallel connection, series connection with the absorber first, and series connection with condenser first. The series connection can be used since both absorber and condenser reject the heat to the same heat rejection stream (but, at different temperature levels). Another important component is the solution heat exchanger between weak solution and strong solution (SHX in Figure 2.5). This heat exchanger is important because, since a strong solution contains heat, it can be transferred to the weak solution. Thus, the heat required in the desorber and the heat that must be removed in the absorber is reduced, increasing the COP of the system. The complete cyclic process of the water/Lithium Bromide absorption cycle is shown in Figure 2.5.

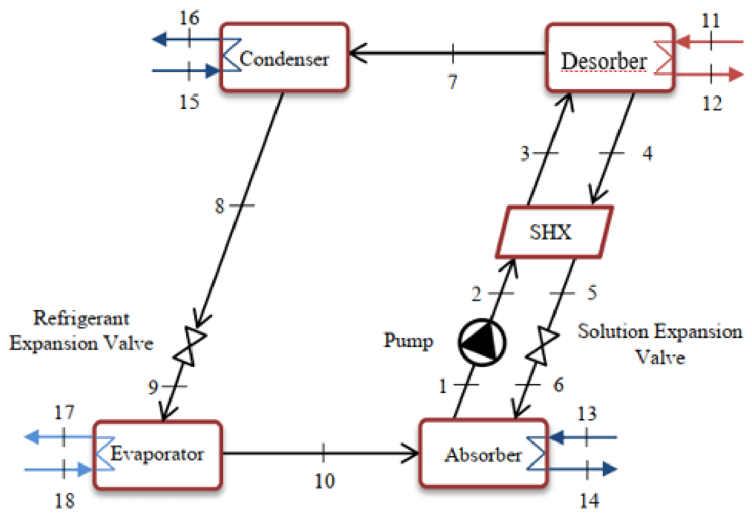

Figure 2.5. Complete system of single-effect water/lithium bromide absorption machine with all the external circuits (Martines Maradiaga, 2013)

2.2.2 Absorption Heat Pump – Reversible Operation

From the description in the previous section, that absorption machine is used to reject the heat at the medium temperature level and also absorb the heat at the low temperature level. The ability to absorb the heat at a low temperature level is utilized during the cooling period (for example: during summer). The absorption machine is called an absorption chiller when the main objective is to provide cooling. However, since the demand in a certain region is not only cooling, it is interesting to use the absorption machine to provide the heating. Thus, it is called absorption heat pump. The reversible operation means that the absorption heat pump can provide cooling and heating by reversing the flow of the end-user circuit. In cooling mode, the flow that enters to the user terminal is the external circuit of evaporator. While in the heating mode, the flow that enters to the user terminal is the external circuit of absorber and condenser. Hence, the system that distribute the energy from the absorption heat pump can be viewed as a heat sink during heating mode and a heat source during cooling mode (Kühn, 2013).

2.2.3 Characteristic Equation of Water/Lithium Bromide Absorption Heat Pump

There are multiple methods to model the absorption heat pump for investigating its performance and operational characteristics. One of the common method is developing the thermodynamic model of the system using energy and mass balances, thermodynamic properties of the working fluid mixture, and heat transfer relationships as it is comprehensively explained in the book of Herold et al. (2016). However, there are other methods such as data-driven modelling of multivariable polynomial regression as it is used by Martinez and Pinazo (2002) to evaluate the COP and cooling capacity of the system.

Another modelling approach that is also used is the characteristic equation method. This method was developed by Hellman et al. (1999) and Zigler et al. (1999) that allows calculating the cooling capacity and the COP of a single effect water/lithium bromide absorption chiller with a simple algebraic equation (Martines Maradiaga, 2013). The simplicity of the application allows the user to have a convenience model regarding the absorption machine that is being investigated.

The absorption machine that will be used is a newly developed absorption machine called BEE from Baelz Automatic with a 50 kW of cooling capacity at the nominal design conditions. This absorption machine has a characteristic equation in the literature that can be used to represent its performance (Albers & Ziegler, 2016). The characteristic equation has been used also during the development of the 10 kW absorption heat pump prototype (Kühn *et al.*, 2010). The characteristic equations of the newly developed 50 kW absorption chiller are:

$$\Delta\Delta t^{*} = t_{Di} \cdot (1 - K_1) - t_{Ai} \cdot (1 - K_2) + t_{Eo} \cdot (1 - K_3) \tag{2.1}$$

$$\Delta\Delta t^{*}_{min} = (t_{Di} - t_{Ai}) - \Delta\Delta t^{*} \tag{2.2}$$

$\Delta\Delta t^{*}$and $\Delta\Delta t^{*}_{min}$ are the characteristic equation in absolute temperature unit of Kelvin, K-values are the characteristic coefficients where K_1 until K_3 is related to the combination between heat transfer in the heat exchanger components and phase equilibrium data of LiBr/H_2O as the working fluid (Albers and Ziegler, 2016). The calculation of driving heat $\dot{Q}_D$ and the cooling capacity $\dot{Q}_E$ of the chiller are:

$$\dot{Q}_E = K_4^{*} \cdot \Delta\Delta t^{*} \tag{2.3}$$

$$\dot{Q}_D = K_5^{*} \cdot \Delta\Delta t^{*} + K_6 \cdot \Delta\Delta t^{*}_{min} \tag{2.4}$$

As it can be seen, the cooling capacity and the driving heat depend on the values of modified characteristic coefficient K_4^{*} and K_5^{*}, while $K_6 \cdot \Delta\Delta t^{*}_{min}$ is the minimum driving heat. The modified characteristic coefficients are obtained from the following equations:

$$K_{Eo} = \frac{1}{1 - (K_1 - K_2) \cdot K_4/\dot{W}_E} \tag{2.5}$$

$$K_4^{*} = K_{Eo} \cdot K_4 \tag{2.6}$$

$$K_5^{*} = K_{Eo} \cdot (K_5 - K_6) + K_6 \tag{2.7}$$

The characteristic coefficient of the absorption chiller can be seen in Table 2.2. The symbol $\dot{W}_E$ is for nominal capacity flow rates of the evaporator's external stream (10 kW/K). The characteristic coefficients are valid only when the capacity rates of all external circuit are at the nominal design condition (Albers and Ziegler, 2016). In this case, the driving hot water outlet temperature and the evaporator external stream inlet temperature can be obtained using these relationships:

$$\dot{Q}_E = \dot{W}_E \cdot (t_{Ei} - t_{Eo}) \tag{2.8}$$

$$\dot{Q}_D = \dot{W}_D \cdot (t_{Di} - t_{Do}) \tag{2.9}$$

where $\dot{W}_D$ is the driving heat capacity flow rate (3.5 kW/K at nominal design condition). The correlation of the heat rejection $\dot{Q}_{AC}$ is not given. However, it is mentioned (Albers and Ziegler,

2016) that further information can be obtained from the BINE information service (2012). Therefore, the heat rejection equation can be included as follows:

$$\dot{Q}_{AC} = \dot{Q}_D + \dot{Q}_E \tag{2.10}$$

$$\dot{Q}_{AC} = \dot{W}_{AC} \cdot (t_{Ai} - t_{Co}) \tag{2.11}$$

Table 2.2. Characteristic coefficient of BEE (Albers and Ziegler, 2016)

Coefficient	Units	Value
K_1	-	0.1
K_2	-	-1.0
K_3	-	-0.1
K_4	kW/K	1.1
K_5	kW/K	1.3
K_6	kW/K	0.1

The amount of heat rejection can be obtained from the global energy balance of the absorption heat pump by assuming that there are no heat losses to the surroundings. Then, the capacity flow rate of rejection medium ($\dot{W}_{AC}$) is calculated from the nominal heat rejection rate divided by the difference between inlet and outlet temperatures of the heat rejection medium. These values (shown in Table 2.3) are taken from BINE information services (2012).

Table 2.3. Nominal design condition of the absorption chiller (type BEE) (BINE, 2012)

Parameter	Absorption chiller (BEE)
Cooling Capacity [kW]	50
Driving Heat [kW]	63
Heat Rejection [kW]	113
Thermal COP	0.79
Chilled Water Temperature (Inlet/Outlet) [°C]	21/16
Hot Water Temperature (Inlet/Outlet) [°C]	90/72
Cooling Water Temperature (Inlet/Outlet) [°C]	30/37
Chilled Water Flow Rate [m^3/h]	8.6
Hot Water Flow Rate [m^3/h]	3
Cooling Water Flow Rate [m^3/h]	14

Using the above characteristic equation, the behaviour of the system based on the external operational conditions (i.e. chilled water outlet temperature, driving hot water inlet temperature, and heat rejection (cooling water) inlet temperature) can be obtained. In other words, the performance data of this machine can be determined.

2.2.4 Performance data of absorption machine based on the Characteristic Equation

In this section, the performance data of the 50 kW absorption machine is shown. It includes the behaviour of the machine as a chiller in cooling mode and as the heat pump in heating mode since it can be used in the reversible operation.

2.2.4.1 The effect of hot water inlet temperature

Figure 2.6 shows the effect of hot water inlet temperature on the cooling capacity and thermal cooling COP of the absorption machine. It is obtained by using the previous characteristic equation with constraining the cooling water inlet temperature and the chilled water supply temperature at the nominal design condition (i.e. 30°C and 16°C, respectively). The hot water inlet temperature of the desorber is varied from 60°C to 100°C. It can be seen in Figure 2.6 that the cooling capacity varies directly proportional to the hot water inlet temperature. Therefore, the higher cooling capacity can be achieved by using higher hot water inlet temperature.

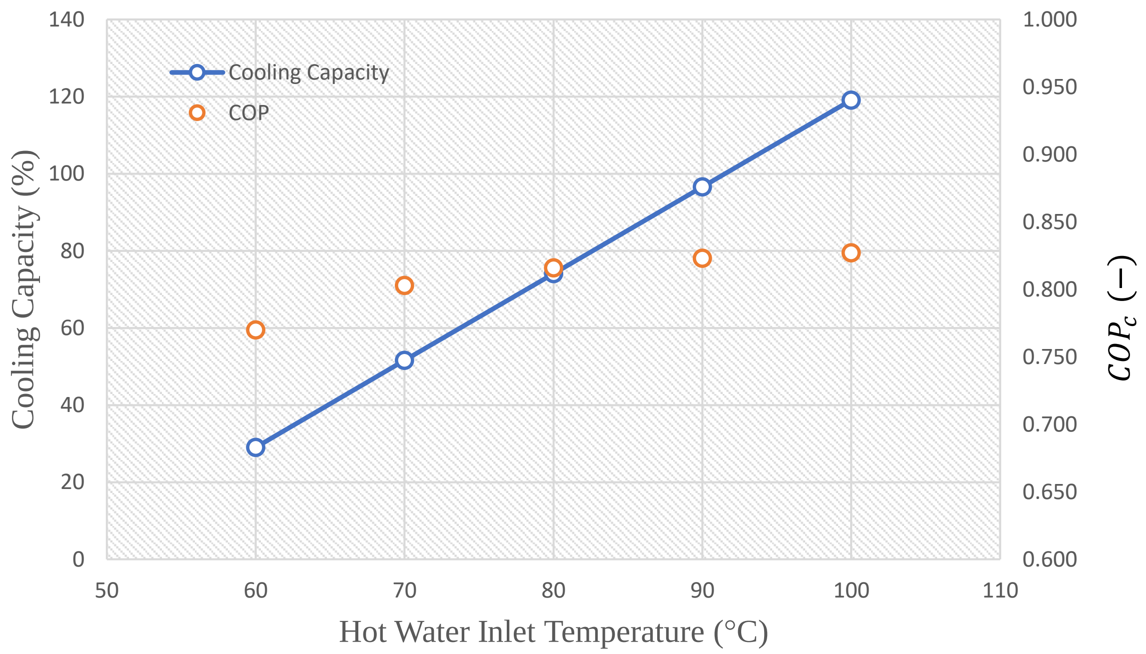

Figure 2.6. Effect of driving hot water inlet temperature on cooling capacity and COP_C

2.2.4.2 Effect of heat rejection medium inlet temperature at different chilled water supply temperature

The cooling demand changes according to several reasons such as occupancy, solar heat gain, and internal heat gain. Another reason is because of the ambient temperature. Higher ambient temperature leads to a higher cooling demand while at the same time reduces the heat that can be rejected (Petersen *et al.*, 2011). The rejected heat also depends on the applied system such as wet, dry, or even hybrid cooling tower. The use of a wet cooling tower for the heat rejection system is commonly chosen because it has good capability to reject the heat in cooling mode as it can provide heat rejection medium inlet temperature below outdoor ambient temperature since it depends on the wet-bulb temperature (Kozlov *et al.*, 2014). In another case, the dry cooler is used because of its allowable operations during the heating season (Kühn *et al.*, 2010). The heat rejection medium (i.e. cooling water) inlet temperature is varied according to its temperature range, that is, 20°C to 40°C (Albers and Ziegler, 2016). The cooling capacity and the thermal COP depending on the cooling water inlet temperature and driving hot water at 90°C are presented in Figures 2.7 and 2.8.

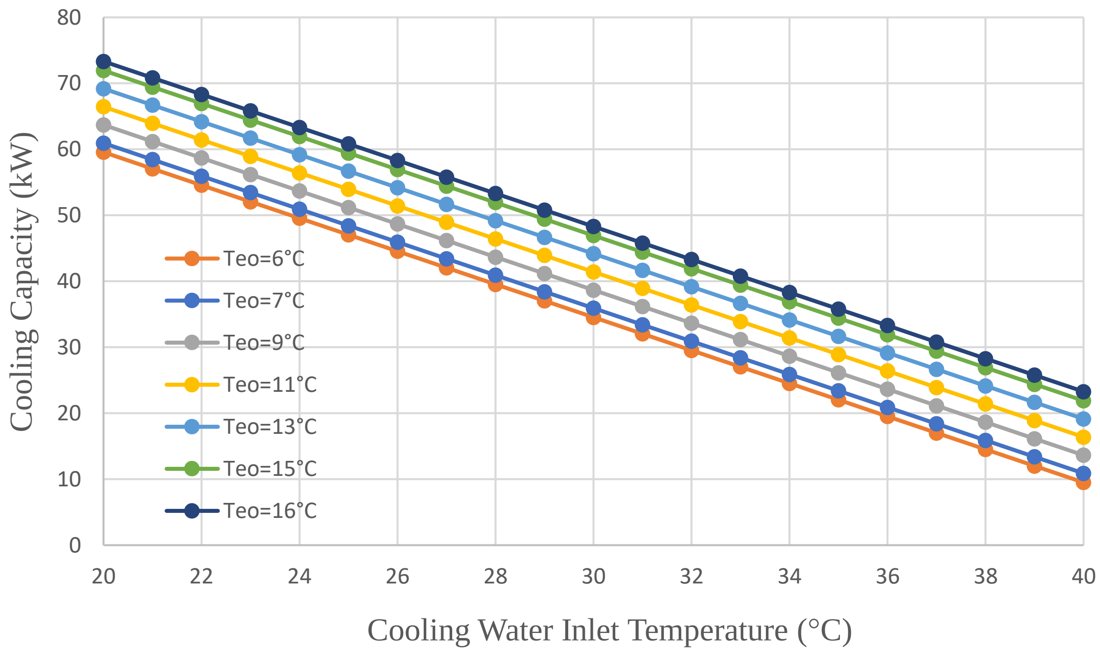

Figure 2.7. Cooling capacity of absorption chiller based on the cooling water inlet temperature

The cooling capacity at a cooling water inlet temperature of 20°C can reach up to around 73 kW or 146% from the nominal capacity with the COP_C of 0.84 at the nominal design condition. Moreover, the absorption chiller still produces 120% of the nominal cooling capacity with a COP of 0.82 at the minimum chilled water supply temperature of 6°C. The minimum cooling capacity at the nominal chilled water supply temperature (t_{EO}=16°C) is 23.3 kW with the COP_C of 0.77. If the minimum cooling capacity is set to be 25% of the nominal capacity, then the system cannot be operated with 6°C chilled water supply temperature in ambient temperature higher than 38°C. It means that in a hot climate system, the absorption chiller cannot be coupled with a dry cooler (Kühn *et al.*, 2010). The COP of the absorption chiller at 6°C supply temperature and cooling water inlet temperature of 38°C is still good (COP_C=0.69).

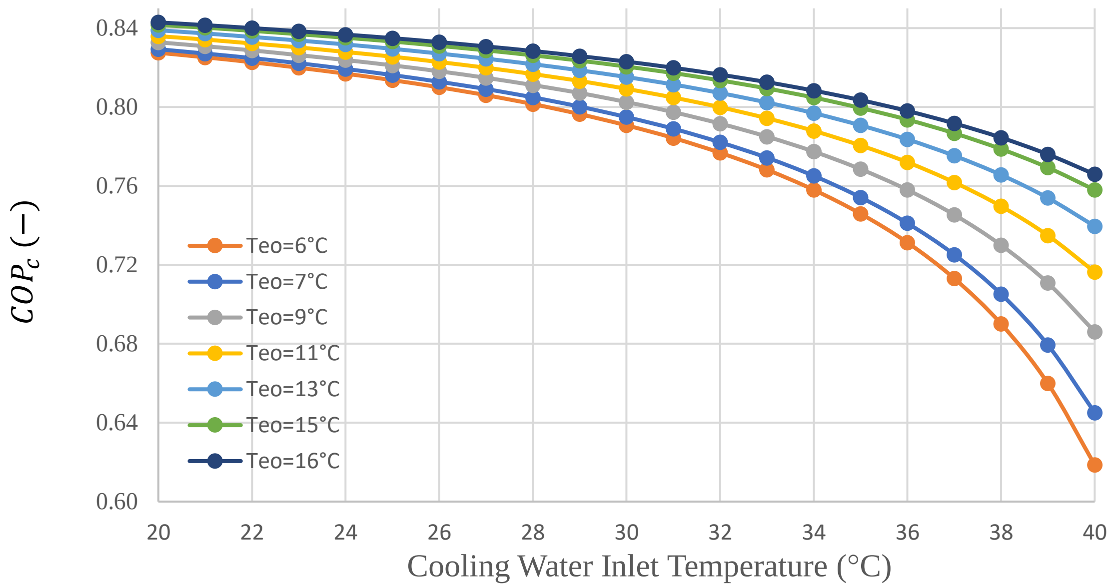

Figure 2.8. COP_C of absorption chiller based on the cooling water inlet temperature

2.2.4.3 Effect of heat source inlet temperature at different heat supply temperature

As it is mentioned in the previous section about the reversible operation, the absorption heat pump is able to supply cold in summer time and heat in winter time (Herold *et al.*, 2016). In the case of cooling mode, the system that distribute the cold in the building is the water circuit that is connected to the evaporator of the heat pump. In heating mode, this water circuit has to be connected to absorber and condenser so that the building can receive heat from the heat pump. In this case, the evaporator should receive heat from other heat source. Several strategies have been developed to choose the heat source such as using dry or hybrid cooler (Asfand *et al.*, 2020), and using the return circuit of the desorber (Güido *et al.*, 2018). The heat source inlet temperature is varied from 10°C to 21°C at different heat supply temperature (T_{CO}) of 30°C, 35°C, 38°C, 40°C, and 45°C. The heating capacity and the thermal COP_H of the heat pump depending on the heat source inlet temperature are presented in Figures 2.9 and 2.10.

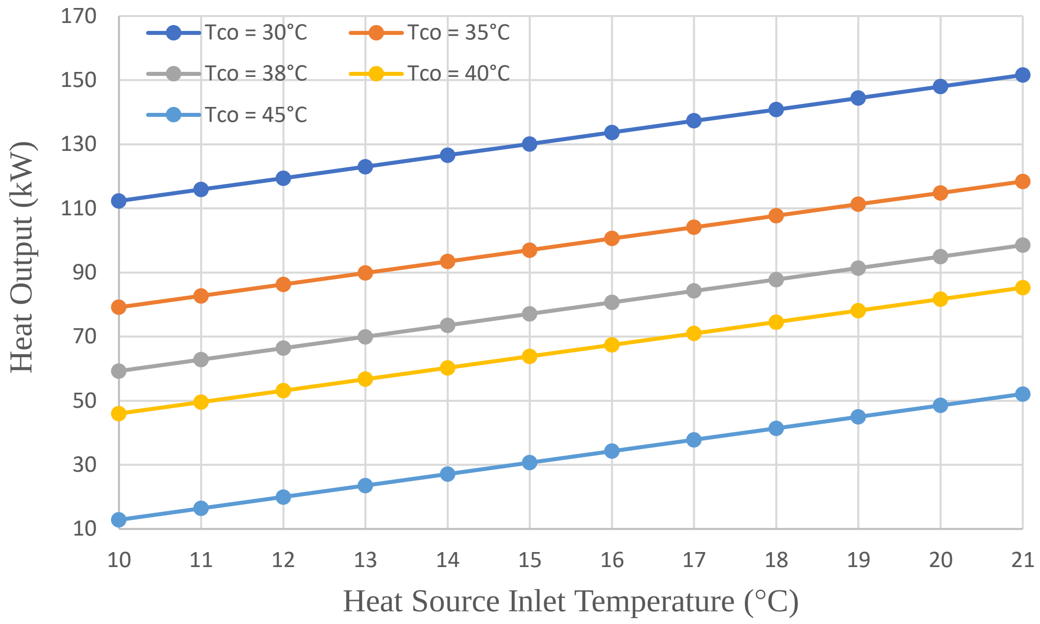

Figure 2.9. Heat output of absorption heat pump based on the heat source inlet temperature

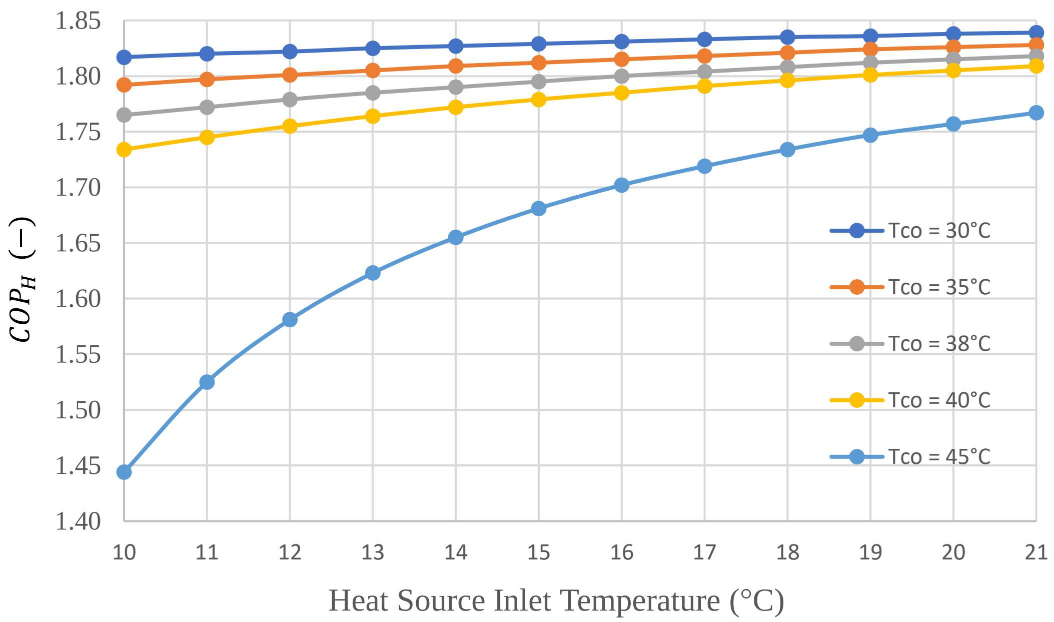

Figure 2.10. COP_H of absorption heat pump based on the heat source inlet temperature

As it can be seen in Figures 2.9 and 2.10, the heat output when heat source inlet temperature of 21°C can reach up to around 150 kW with the COP_H of 1.84 at hot water supply temperature of 30°C, while the heat capacity is still above 110 kW when the heat source inlet temperature is 10°C at the same hot water supply temperature. It is obvious that the higher the hot water supply temperature, the lower the heat capacity. The minimum heat capacity at the maximum allowed hot water supply temperature (i.e. t_{CO}=45°C) is 12.84 kW with the COP_H

of 1.76. At this point, the driving energy used is very low and thus the return temperature of the driving hot water is still high. This condition can be avoided by increasing the hot water inlet temperature or lowering the hot water supply temperature (Kühn, 2013).

Regardless of all the simplicities, the use of the characteristic equation of the absorption chiller in the nominal condition results in the different values of all the heat transfer rates that are shown in Table 2.4. However, the deviation of the results in the nominal condition does not exceed more than 10% from the nominal design values reported in the literature (BINE, 2012). The comparison of results obtained from the characteristic equation is also compared with the manufacturer's catalogue (Baelz Automatic, 2019) as is illustrated in Table 2.5. It shows that the COP deviation is getting higher when the hot water inlet temperature is not in at the nominal design temperature (i.e., 90°C), with the highest deviation of around 16.5% corresponds to the lowest hot water inlet temperature of 60°C.

Table 2.4. Comparison between characteristic equation method (ChEM) predictions and the corresponding data of BINE (2012)

Heat transfer	ChEM	Nominal Data (BINE, 2012)	Deviation (%)
Cooling Capacity (kW)	48.3	50	3.4
Driving Heat (kW)	58.7	63	6.83
Heat Rejected (kW)	107	113	5.31
COP	0.82	0.79	3.80

Table 2.5. Comparison between characteristic equation method predictions and corresponding manufacturer's data at different driving hot water inlet temperatures

t_{Di} (°C)	$\dot{Q}_E$ (kW)	$\dot{Q}_{E,Actual}$ (kW)*	Deviation of $\dot{Q}_E$ (%)	COP (-)	COP_{Actual}* (-)	Deviation of COP (%)
60	14.52	13.65	6.34	0.770	0.661	16.490
70	25.78	24.85	3.74	0.803	0.751	6.924
80	37.04	38.26	3.19	0.816	0.793	2.900
90	48.30	50	3.39	0.823	0.802	2.618
100	59.55	63.4	6.07	0.827	0.793	4.288

* Catalogue data of absorption chiller (type BEE -50 kW) (Baelz Automatic, 2019)

2.3 Estimation of Space Cooling and Heating Demand

Space cooling and heating demand are important as a key indicator of energy consumption of the building. The size of heating and cooling equipment, in this case, an absorption heat pump, is determined based on the desired indoor conditions that must be kept according to an environmental condition in the specific location of the building (Cengel and Ghajar, 2002). According to ASHRAE (2013a), there are several options to estimate the space cooling and heating demand of buildings. From the steady state approach up to the model simulation. The steady state approach includes simple linear regression, multiple linear regression, degree-days method, and bin method. While the model simulation includes computational simulation with energy modelling software such as EnergyPlus (DOE, 2017) and TRNSYS (TRNSYS16, 2007).

2.3.1 Degree-Day Method

Degree day (DD) is an indicator based on climatic data that can be used to determine the energy demand of the buildings (Ciulla et al., 2015). According to CIBSE (2006), this method has the origins in agricultural research where the variation of outdoor air temperature is important, and the concept is easily transferable to building energy estimation. Moreover, this method is considered the simplest and most intuitive way to estimate the energy use of a building in a steady-state approach (ASHRAE, 2013a). A degree-day is a difference between the outdoor air temperature and the base temperature over a specific period. In the present case, degree-day represents how big is the difference between the outdoor air temperature and the base temperature over the day and it is expressed as follows:

$$DD_H = \frac{\sum_{o=1}^{24}(T_b - T_{amb})^+}{24} \tag{2.12}$$

$$DD_C = \frac{\sum_{o=1}^{24}(T_{amb} - T_b)^+}{24} \tag{2.13}$$

where DD_H and DD_C are the degree-day for heating and cooling, respectively. T_{amb} is the ambient air temperature and T_b is the base temperature. The positive sign means that the value of degree-days only be considered when the ambient air temperature is lower than the base temperature for heating and the reverse for cooling. The ambient air temperature and the base temperature are evaluated every hour to obtain more precise result. Thus, the degree-day is the average value in 24 hours (ASHRAE, 2017).

2.3.2 Base Temperature

The base temperature is a fundamental notation that corresponds to the relationship between climate, occupancy, building construction, and the heat gain in the building. It is the outdoor temperature below the setpoint temperature at which the indoor temperature is in comfortable range without heating or cooling (Bhatnagar, Mathur and Garg, 2018), and this comfortable condition is satisfied when the total heat loss of the building is balanced by the total heat gain of the building. The energy balance of this condition is expressed as follows:

$$Total\ Heat\ Loss\ of\ The\ Building = Total\ Heat\ Gain\ of\ The\ Building \tag{2.14}$$

$$HLC \cdot (T_b - T_{in}) = \dot{Q}_G \tag{2.15}$$

where HLC is the total heat loss coefficient of the building in kW/K (which will be explained in detail in the following section), T_{in} is the indoor temperature, T_b is the base temperature, and $\dot{Q}_G$ is the total heat gain of the building in kW. The total heat gain of the building is evaluated from the solar heat gain through the glazing surface in the building and the internal heat gain which corresponds to the occupancy, lighting, and equipment of the building. Then, the definition of base temperature is:

$$T_b = T_{in} - \frac{\dot{Q}_G}{HLC} \tag{2.16}$$

In cold weather, the building loses heat to the environment. This heat is partly replaced by the solar heat gain and the internal heat gain, while the rest is supplied by the heating device. Since the heat gains contribute to the heating of the building, there is an outdoor temperature below the set-point temperature, at which the heating system should not be operated. That is the base temperature. The conceptual understanding is similar also to the hot season. When the outside temperature is considered as the base temperature, the solar heat gain in the building only consists of direct beam solar heat gain and diffuse solar heat gain. The conductive heat gain is not considered as the outside temperature is lower than the inside temperature, so the conductive heat gain is considered as heat loss. Therefore, the solar heat gain is calculated as follows (ASHRAE, 2017):

direct beam solar heat gain (q_b):

$$q_b = AE_{t,b}SHCG(\theta)IAC(\theta, \Omega) \tag{2.17}$$

diffuse solar heat gain q_b:

$$q_d = A(E_{t,d} + E_{t,r})\langle SHCG\rangle_D IAC_D \tag{2.18}$$

total solar heat gain (Q_{sol}):

$$Q_{sol} = q_b + q_d \tag{2.19}$$

where A is the window area, $E_{t,b}$, $E_{t,d}$, and $E_{t,r}$, is the beam, sky diffuse, and ground-reflected diffuse irradiance, respectively, $SHCG(\theta)$ and $\langle SHCG\rangle_D$ are the Beam and Diffuse Solar Heat Gain Coefficient, while $IAC(\theta,\Omega)$ and IAC_D are indoor solar attenuation for the beam and diffuse solar heat gain. In the present study, the building is considered without a shading device, so the values of $IAC(\theta,\Omega)$ and IAC_D are considered one.

As it can be seen, the calculation of direct beam and diffuse solar heat gains need their respective SHCG values. However, the window manufacturers normally provide the Total Solar Heat Gain Coefficient ($SHCG_{Total}$) of the window (Cengel and Ghajar, 2002). Therefore, the calculation of solar heat gain is simplified as:

$$Q_{sol} = q_b + q_d = AE_{Total}SHCG_{Total}GFR \tag{2.20}$$

where E_{Total} is total solar irradiance to the window and GFR is the glazing-frame-ratio. In the building installation, the window consists of glass and a frame to hold the glass. In this case, normally the frame will cover some area of glass so that the glazing surface is reduced. The glazing-frame-ratio is the ratio between the glazing area and the frame area. In this case, the typical glazing-frame-ratio is considered to be 0.9 (Harvey, 2020).

2.3.3 Heat Loss Coefficient

Heat loss coefficient (HLC) is the coefficient that corresponds to the total rate of heat loss from the building per indoor-to-outdoor temperature difference (Harvey, 2020). It is the sum of the U-factor multiplied by the area for the external surface of the building, such as walls, windows, roof, and losses from infiltration and ventilation. It is computed as:

$$\mathrm{HLC} = \sum A_i U_i + \frac{\rho C_p N \cdot V}{3600} + \rho C_p \dot{V}_m (1 - e_m) \tag{2.21}$$

where A_i is the area of any external surface of the building and U_i is the corresponding thermal transmittance in W/m^{2}K, ρ is the density of the air (1.25 kg/m^3), C_p is the air specific heat capacity (1005 J/kg-K), N is air infiltration with the number of air change per hour, V is the unit volume of the building (m^3), $\dot{V}_m$ is the volumetric flow rate of air in the ventilation, and e_m is the heat recovery effectiveness of the heat exchangers between fresh air that enters the building with the outgoing air from inside to outside of the building.

The volumetric flow rate can be considered from the minimum constant ventilation air required according to a building standard. One of the standards that can be used is ASHRAE standards 62.1-2019 (ASHRAE, 2019) which can be seen in Table 2.6 for an office building.

For the recovery heat effectiveness of the heat exchanger, the effectiveness of a fixed plate heat exchanger normally has sensible heat recovery between 0.5 to 0.8 (Sammeta *et al.*, 2011). Moreover, the effectiveness of the new system was found to be about 0.75 for sensible recovery and 0.65 for latent recovery (Nasif *et al.*, 2010). Latent recovery depends on the relative humidity the between environment and indoor conditions. High tolerance in relative humidity is often reported by some research (Hwang *et al.*, 2006). Therefore, the consideration of sensible heat recovery effectiveness is sufficient depending on the approach. The general typical nominal value of 0.7 effectiveness has been assumed for heat recovery device for mechanical ventilation. This value has been widely chosen because, although there is no European recommendation for the minimum effectiveness for heat recovery device of mechanical ventilation, the recommended value of at least 0.7 has been recommended for countries such as Denmark, Sweden, and Italy (Tafelmeier *et al.*, 2017).

Table 2.6. Required minimum ventilation air flow rate for office building (ASHRAE, 2019)

Occupancy Category	People Outdoor Air Rate		Area Outdoor Air Rate	
	Cfm/person	L/s.Person	Cfm/ft^2	L/s.m^2
Breakrooms	5	2.5	0.12	0.6
Main entry lobbies	5	2.5	0.6	0.5
Occupiable storage rooms for dry materials	5	2.5	0.6	0.5
Office Space	5	2.5	0.6	0.5
Reception areas	5	2.5	0.6	0.5
Telephone or data entry	5	2.5	0.6	0.5

The U value is taking into account the conduction and convection heat transfers from the building to the outside environment. This is because the base temperature is always lower than the thermostat temperature. In a practical case, the thermal resistance of the layer of the building envelope R_i is more common in the building technical data rather than the thermal transmittance. In this case, the relation between R_i and U_i is expressed as follows (López-Ochoa *et al.*, 2020):

$$R_{total,i} = R_{si,i} + \sum_{n} R_i + R_{se,i} \tag{2.22}$$

$$U_i = \frac{1}{R_{total,i}} \tag{2.23}$$

where $R_{si,i}$ and $R_{se,i}$ are the surface thermal resistance of the thermal envelope *i* of the building for indoor air and outdoor air, respectively, in $m^2 \cdot K/W$. While $R_{total,i}$ is the total thermal resistance of the façade *i* in the building. The value of $R_{si,i}$ and $R_{se,i}$ are different according to the position of the element i and the direction of the heat flow. According to the Spanish Ministry of Development (Ministerio de Fomento, 2015), $R_{si,i}$ and $R_{se,i}$ are listed in Table 2.7.

Table 2.7. Thermal resistance of the thermal envelope *i* for indoor and outdoor air (Ministerio de Fomento, 2015)

Position of the element i	Figure	$R_{se,i}$	$R_{si,i}$
Vertical walls or with a slope above the horizontal > 60° and Horizontal flow	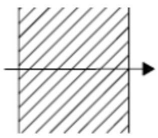	0.04	0.13
Horizontal walls or with a slope above the horizontal ≤60 ° and upward flow (Roof)	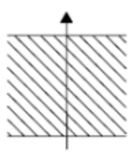	0.04	0.10
Horizontal enclosures and downward flow (Floor)	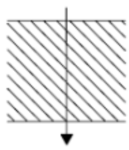	0.04	0.17

2.3.4 Energy Demand Estimation

From the definition of base temperature, it follows that the heat loss coefficient multiplied by the degree day will give the heating or cooling demand, that is, the required amount of heat supplied and/or removed from the building. The amount of heating and cooling demand is obtained as follows:

$$Demand\ (kW) = HLC \cdot DD \tag{2.24}$$

where DD is the degree day that corresponds to DD_H for heating demand and DD_C for cooling demand. In the ASHRAE handbook fundamentals (ASHRAE, 2013a), the energy consumption of the building from cooling and heating operation can be obtained by including the efficiency of heating and cooling device. The utilization of degree day method is limited to the energy demand estimation only. Moreover, energy demand estimation with degree-days only takes into account sensible heat (temperature difference). Thus, the appropriate cooling and heating application in order to make the calculation more accurate is by using the device that only rely on sensible heat, such as chilled beam ceilings or walls, and radiant ceiling, wall, or floor heating (CIBSE, 2006).

In this master thesis, the district heating design temperature that has been mentioned in this chapter will be used as the desorber hot water inlet temperature of the absorption heat pump. The absorption heat pump, in this case the newly developed single-effect water/lithium bromide absorption machine (type BEE-50 kW_{cold}), will be used to cover the space heating and cooling demand of the selected building. The space heating and cooling demand are estimated based on the degree-days method which also has been explained briefly. The overall methodology for this master thesis is explained in chapter 3.

3. METHODOLOGY

3.1 Heating and Cooling Demand Estimation

In this study, the estimation of heating and cooling demand with the degree-days method that has been explained in chapter 2 is applied to estimate the demand in the reference non-residential building (i.e., small office building) model developed by the U.S Department of Energy (Deru *et al.*, 2011). The building is exposed to a typical metrological year weather data for two cities in two different European countries. The selected European countries are based on the availability of district heating where the information of design district heating is on subchapter 2.1.4. and the climate region of the countries based on the map of climate areas in Europe EUCA15000 (Schneider *et al.*, 2013). The countries are Spain and Germany where the corresponded cities are Barcelona and Berlin. It can be seen from Figure 3.1 that Spain is in the Mediterranean climate region and German is in the Temperate climate region. The Mediterranean region has mild and wet winters, hot and dry summers, and clear skies for almost along the year, while the temperate climate has colder winters and warmer summers.

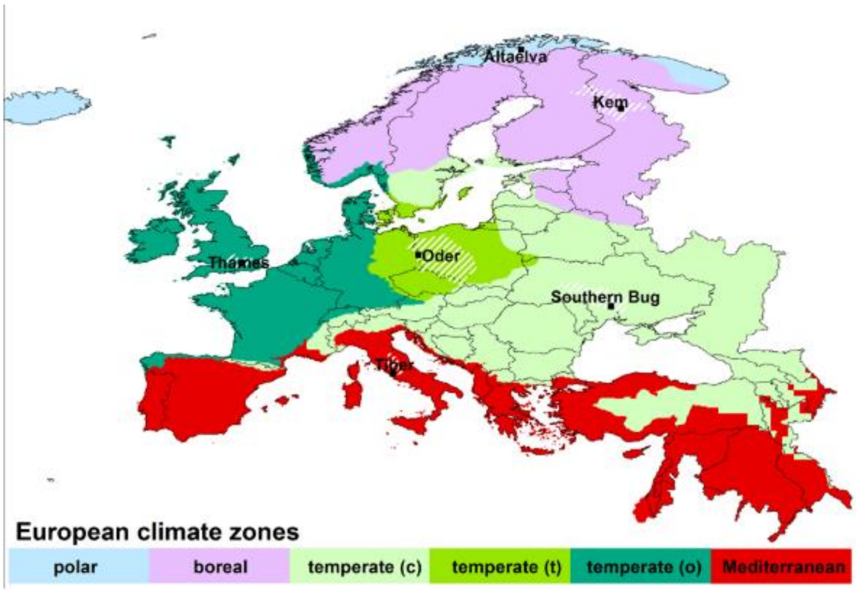

Figure 3.1. European climate region (Schneider et al., 2013)

The metrological year weather data for Barcelona and Berlin are obtained from the EnergyPlus software (EnergyPlus, 2016). The data from the EnergyPlus for Barcelona and Berlin weather data were derived from IWEC. The construction of this meteorological archive takes into account historical climatic data from meteorological stations located within the perimeter of the cities. It can be seen in Figure 3.2 that both cities have a significant difference in ambient temperature. In the winter period, the lowest temperature in Barcelona is 1°C while in Berlin can reach until −9°C. However, in the summer period, Berlin's ambient temperature can reach up to 32°C while Barcelona only until 31°C. In Berlin, the ambient temperature drops significantly at night where it can be as low as 9°C. The hottest month for Berlin is in June while in Barcelona is in August.

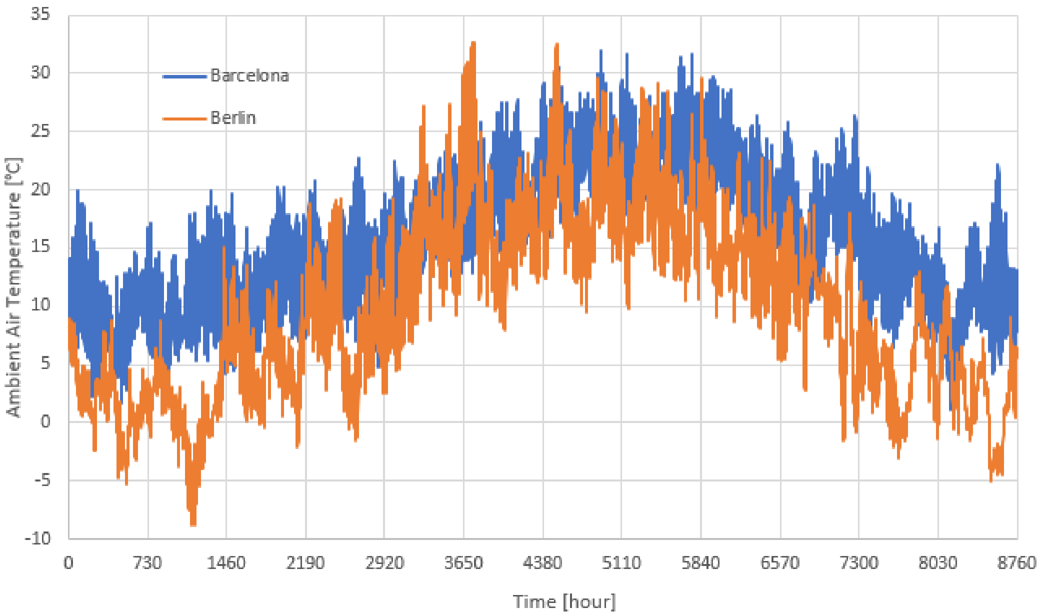

Figure 3.2. Hourly ambient air temperature of Berlin and Barcelona

3.1.1 Building Description

The building is a 1-floor typical small office building constructed in the post-1980. It consists of 1 core zone with an area of 224 m^2 and 4 perimetric zones where the south and north zone have an area of 169 m^2 while the east and west zone has an area of 100 m^2. Table 3.1 summarizes basic information about the reference office building considered in the present research and Figure 3.3 shows the building model**.** The volume of the building is 3400 m^3 and the infiltration rate is 1.68 ACH.

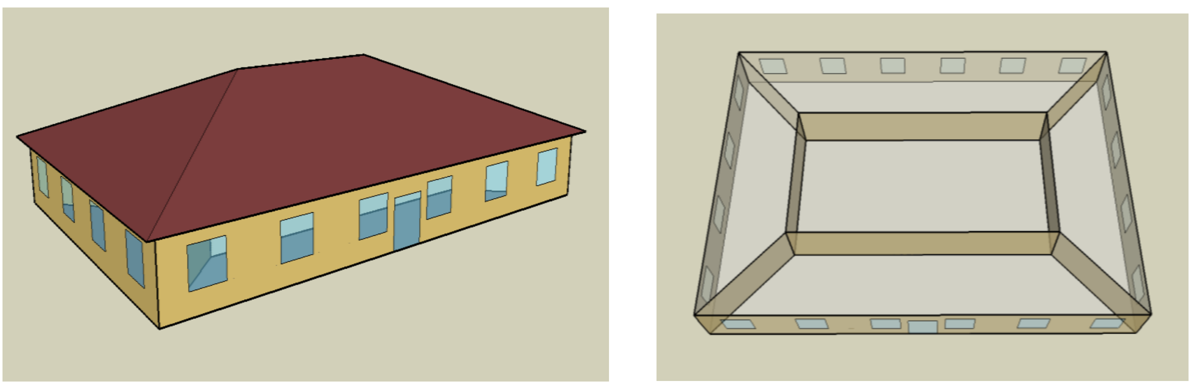

Figure 3.3. Typical 1 floor small office building (US Department of Energy, 2012)

Table 3.1. Characteristic of typical Small Office Building

Building Components	Type	Area (m^2)	Thermal Properties	
Exterior Walls	Mass Wall	336	R-Value (m^2K/W)	1.37
Roof	Attic	853		3.24
Floor	Mass Floor	762		0.54
South Window	Glazing	24.91	U-Value (m^2K/W) and SHGC	4.21 and 0.37
North Window		24.91		
East Window		16.56		
West Window		16.56		

3.1.2 Building Heat Loss Coefficient Calculation

As the calculation is following the procedure in subchapter 2.3.3, the element (i) of the building consists of the roof, external walls, floor, and window. The R-value is available for the roof, external walls, and floor, while the window has directly the U-factor. The other parameters have also been considered in that subchapter (density and heat capacity of air, infiltration rate and ventilation flow rate, heat exchanger effectiveness). Thus, the calculation can be carried out and the results are provided in Table 3.2.

Table 3.2. Heat Loss Coefficient Calculation

Variables	Walls	Roof	Floor	Window
$R_{si,i}$ (m^2K/W)	0.13	0.1	0.17	-
R_i (m^2K/W)	1.37	3.24	0.54	-
$R_{se,i}$ (m^2K/W)	0.04	0.04	0.04	-
$R_{total,i}$ (m^2K/W)	1.54	3.38	0.75	-
U (W/m^2K)	0.65	0.29	1.33	4.21
AU (W/K)	218.23	252.50	1016	349.3
HLC (kW/K)		3.87		

As it can be seen, the biggest thermal transmittance corresponds to the window. It means that the biggest heat loss is transmitted through the window. The total heat loss coefficient is 3.87 kW/K, which means that the building will lose 3.87 kW of heat per 1 K difference between outdoor air temperature and the balance temperature. This value is considered a constant value along the year and the value will be the same in every area since there is no weather factor in the calculation procedure.

3.1.3 Building Heat Gain Calculation

The heat gain of the building consists of internal and external gains. The internal gains are the heat gain from inside the building such as lighting, occupancy, and the equipment available in the building. In this case, all the internal heat gains are considered from the newest ASHRAE handbook in 2017 (ASHRAE, 2017). While the external gains are the solar radiation transmitted through the glazing of the external surface of the building. In this case, the building has a glazing surface in every external wall and the building does not have a skylight.

3.1.3.1 Internal Heat Gain

The factors considered for the internal heat gain are listed in Table 3.3. As it can be seen, the heat generated by the equipment corresponds to one of the scenarios proposed by ASHRAE (2017) which is the office that has 2 screen projector, 1 printer every 10 workstations, and 1 laptop in every 11.06 m^2 each workstation. Moreover, with this scenario, it can be assumed that 1 workstation is occupied by 1 person (11.06 m^2/person). 1 person generates 75 W of sensible heat during moderately active office work.

Since the core zone is surrounded by the perimetric zones, it can be considered as an enclosed zone. The perimetric zones have a window to the ambient so the light can be transmitted to the zone during the day, thus the perimetric zone can be considered as an open-plan zone. In this case, according to ASHRAE, the lighting requirement for the open-plan and enclosed are different. The lighting system in an enclosed zone typically generates 12 W of heat while an open-plan office generates 10.6 W of heat.

Table 3.3. Heat generated by people, lighting, and equipment (ASHRAE, 2017)

Maximum Internal Heat Gain	**Value**
People (W/person)	75
Lighting (W/m^2)	12 and 10.6
Equipment (W/m^2)	9.06

According to data listed in Table 3.3 and the corresponding building characteristic in Table 3.1, The maximum internal heat gain for this building is 20.5 kW. The internal heat gain varies according to the schedule as a function of the maximum internal heat gain fraction. In this case, the schedule for people, lighting, and equipment are adapted from ASHRAE standards 90.1-2013 (ASHRAE, 2013b). The schedules consist of weekday, Saturday, and Sunday, as can be seen in Figures 3.3 to 3.5.

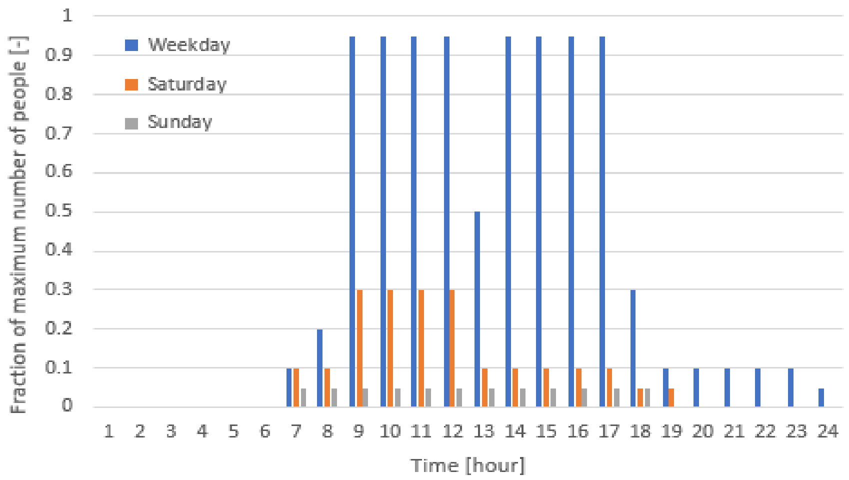

Figure 3.4. People Occupancy Schedule

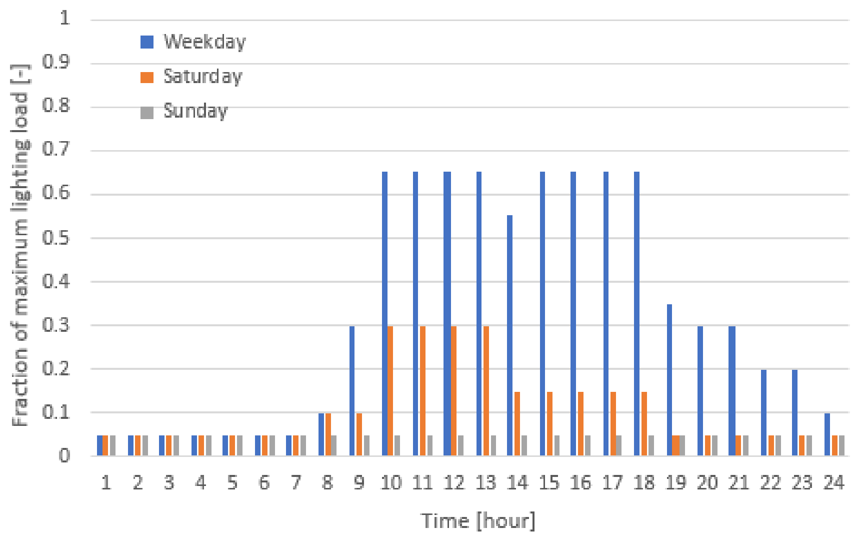

Figure 3.5. Lighting Schedule

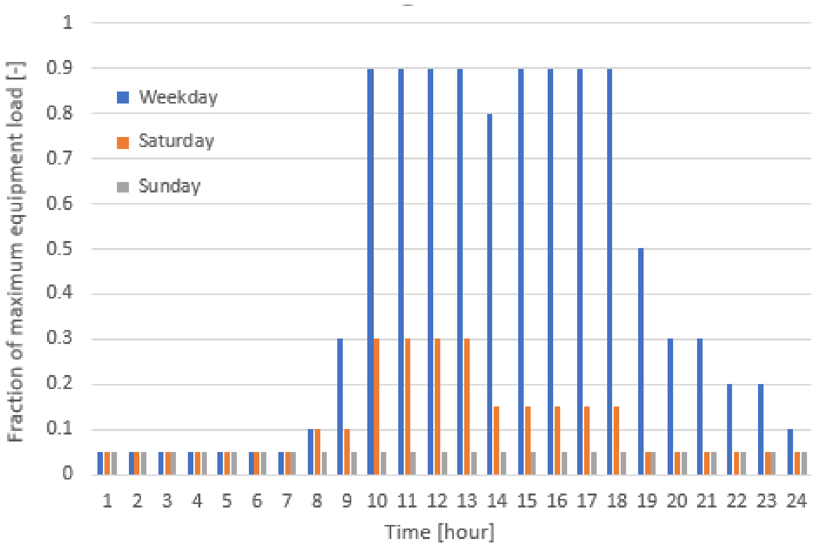

Figure 3.6. Equipment Schedule

3.1.3.2 Solar Heat Gain

The total solar irradiance to the building is obtained from TRNSYS software (TRNSYS16, 2007) by using the metrological data of Berlin and Barcelona and by defining the orientation and the angle of the glazing surface. In this case, the building is assumed to face the equator, and the glazing surface (which also part of the wall) is 90° facing the azimuth. The glazing surface area is considered as shown in Figure 3.7. The values obtained in TRNSYS is transferred to excel to perform the calculation of the solar heat gain using equation 2.20 in subchapter 2.3.2. The results are shown in Figures 3.8 and 3.9.

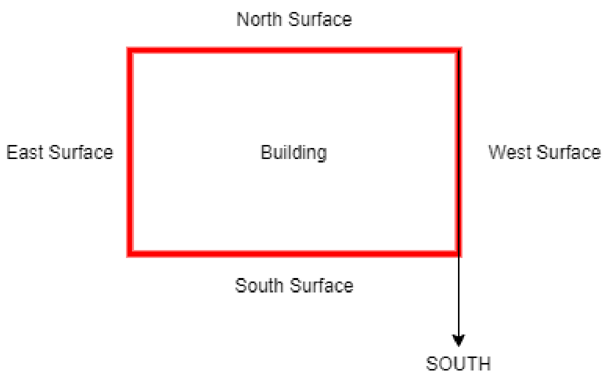

Figure 3.7. Building Orientation

3.1.4 Base Temperature and Degree-Day Calculation

Since the building heat loss coefficient and total building heat gains have already been obtained, the base temperature can be obtained by using equation 2.16 in subchapter 2.3.2. The difference between base temperature for cooling and heating is on the set point temperature. In this case, the set point temperature changes according to the schedule provided by the reference building itself (US Department of Energy, 2012). In cooling mode, the set point temperature for the building is 24°C during occupied hours and 27°C during non-occupied hours. While in heating mode, the set point temperature for the building is 21°C during occupied hours and 16°C during non-occupied hours. This set point temperature for building can be used widely in the world as it is a typical set point temperature. The hourly result for base temperature calculation can be seen in Figures 3.8 and 3.9 for the first week of the year. It can be seen that base temperatures change according to time because of different heat gain and set point temperature in each hour. In the first week of the year in Berlin, the ambient temperature is always lower than the heating base temperature, thus the building always needs heating in this period. While in Barcelona, there are conditions when the ambient temperature is in between heating and cooling base temperature. In this condition, the building does not have heating nor cooling demand. But there is also a small part of the condition when cooling is required, that is when the ambient temperature is higher than the cooling base temperature. The cooling and heating degree days are determined according to equations 2.12 and 2.13 in subchapter 2.3.1. Finally, after calculating the heating and cooling degree days, the space heating demand and cooling demand can be obtained. The results of the heating and cooling demand are presented and discussed in chapter 4.

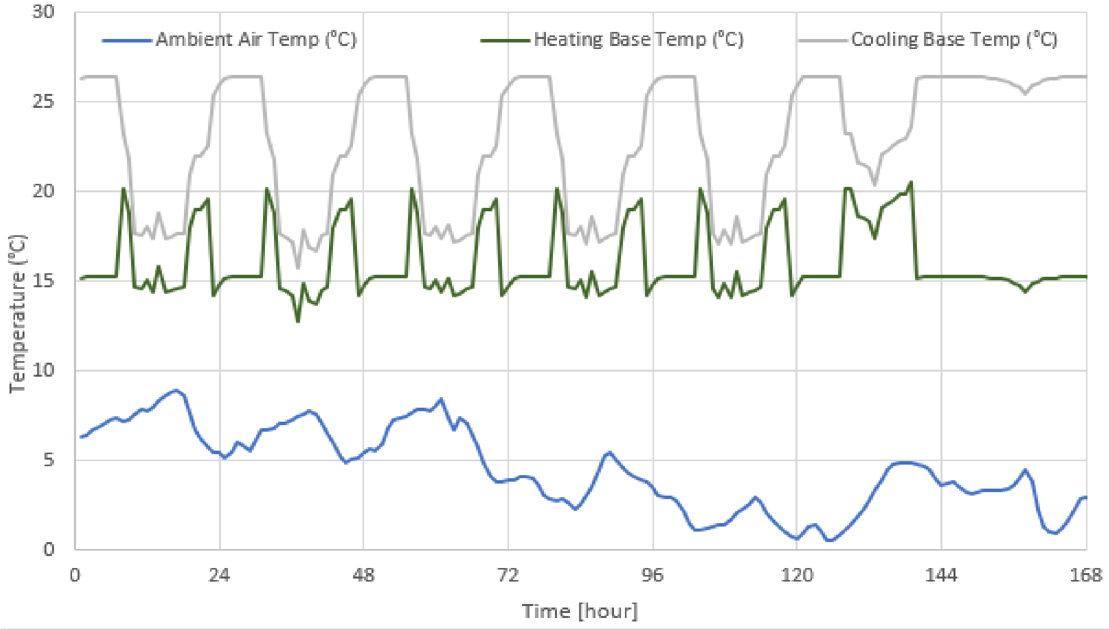

Figure 3.8. Changes of Ambient Air Temperature, Heating Base Temperature, and Cooling base Temperature in the first week of the year for Berlin

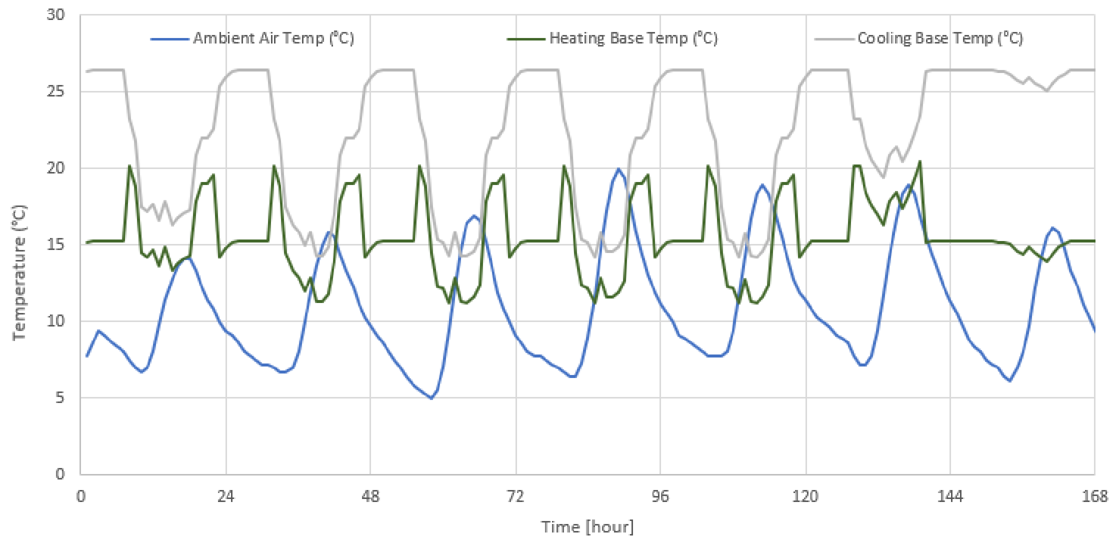

Figure 3.9. Changes of Ambient Air Temperature, Heating Base Temperature, and Cooling base Temperature in the first week of the year for Barcelona

3.2. System Description

The schematic diagram of the proposed system for the provision of space cooling and heating for an office building using a district heating network driven water/lithium bromide absorption chiller is illustrated in Figure 3.10. The absorption chiller (i.e., BEE-50 kW) is used to cover the space cooling and heating demand of the building in Berlin and Barcelona through reversible operation in cooling mode and heating mode. The HVAC system of the building is assumed to be a chilled ceiling with a constant supply temperature of 16°C in cooling mode and floor heating with a supply temperature between 30°C and 40°C in the heating mode. This assumption is taking into account the degree-days estimation method that does not consider humidification and dehumidification (CIBSE, 2006). The reversible operation is controlled by opening and closing the valve according to the mode of operation. During cooling mode, the chilled water from the evaporator external stream outlet will pass through valve-1 to cover the cooling demand. After that, the chilled water will be recirculated to enter the absorption chiller through the inlet of the evaporator external stream. The cooling water from the condenser's external stream outlet will pass through valve-2 to the dry cooler. In this case, the dry cooler will handle the heat rejection to the ambient. Valve-3 will be used to ensure the cooling water inlet temperature of the absorber is not lower than the minimum allowed temperature of the absorption chiller.

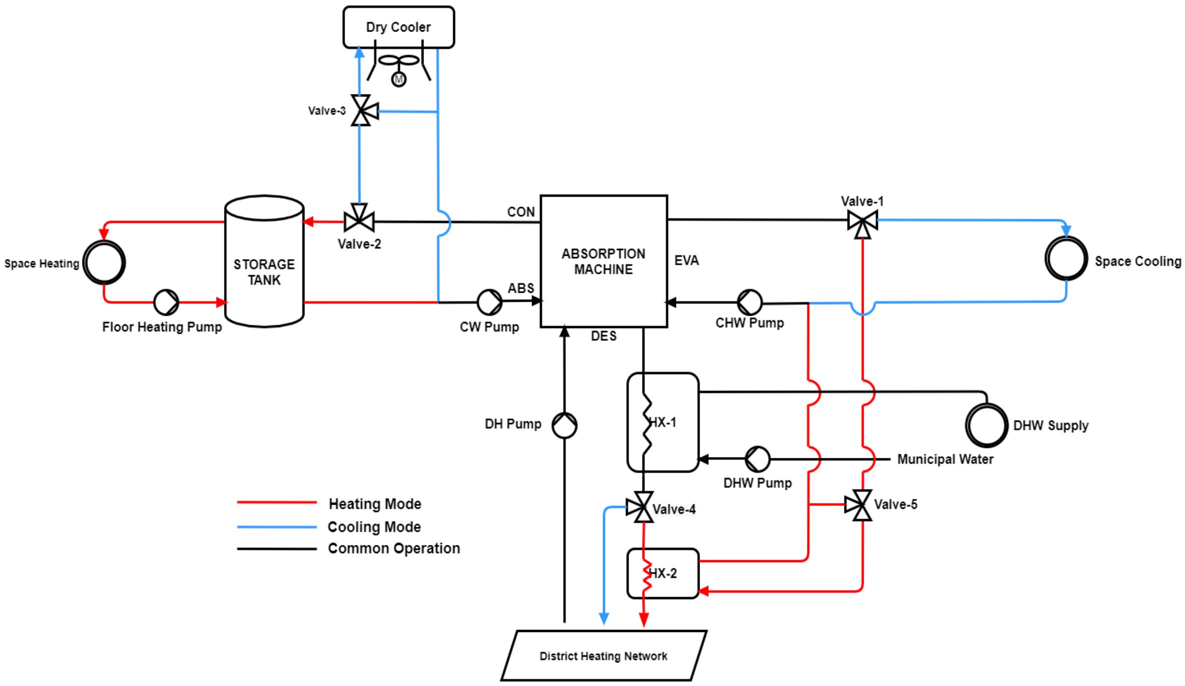

Figure 3.10. Schematic Diagram of the Proposed System

In the heating mode, valve-1 will pass the water from the evaporator to the heat exchanger-2 (HX-2). The heat will be transferred to the chilled water in the HX-2. Valve – 5 will divert the flow to mix it with the outlet of HX-2 to ensure the evaporator's external stream inlet temperature does not exceed more than the maximum allowed temperature, that is 21°C. After that, the chilled water will go to the inlet of the evaporator to be a heat source for the absorption machine. The water from the outlet of the condenser will pass through valve-2 to enter the storage tank. After that, the water will be recirculated to enter the absorption chiller at the inlet of the absorber external stream. The space heating demand will be covered by the secondary circuit of the storage tank. Since the useful heat from the absorption machine is high, the storage tank is used as a buffer to store the heat from the absorption machine. Thus, the heating demand can be covered without operating the absorption machine.

In both modes of operation, the domestic hot water is produced by HX-1, which increase the municipal water temperature to the desired hot water temperature, in this case, it is assumed as 60°C.

This system (Figure 3.10) is using the district heating network as the driving heat source of the absorption heat pump. The hot water in the outlet of the desorber external stream will enter the HX-1 to produce domestic hot water. In the heating mode, the hot water will pass through valve-4 to go to HX-2. In HX-2, the hot water releases heat, and the heat is transferred to the heat source circuit. After that, the hot water will go to the return flow of the district heating network. In cooling mode, valve-4 will pass the water directly to the district heating network since the HX-2 will not be used in cooling mode.

3.3 Annual Simulation of The System

The system is simulated by using TRNSYS software (TRNSYS16, 2007) with two separate simulations, in cooling mode and heating mode. The main components, as well as the input of the components in both modes of operation, are as follows:

- Weather data file – Type 15-3

  Type 15-3 is used to read and interprets weather data file. In this case, it is used to read weather data file in Berlin and Barcelona.
- Space cooling and heating demand file – Type 9c

Type 9c is used to read cooling and heating demand data that has been previously estimated for the building, using degree days method, in Berlin and Barcelona.

- External Circuit Pumps – Type 114

  Type 114 is a single speed pump that is used as an external circuit pumps such as cooling water pump, chilled water pump, and hot water pump. In this case, the volumetric flow rate of the pumps is defined from the catalogue data of the Absorption Chiller (BEE-50 kW (BINE, 2012)) as it can be seen in Table 3.4.

Table 3.4. External Circuit Pumps Flow

Pumps	Flow of the pumps (m^3/h)
Cooling Water Pump	14.4
Chilled Water Pump	8.5
Hot Water Pump	3.0

The hot water pump will pump the district heating water with a constant temperature of design district heating temperature is Berlin and Barcelona, that is, 80°C and 90°C, respectively.

- Absorption Chiller of BEE 50 kW – Type 107

  Type 107 is a standard component for simulating single-effect hot water fired absorption chiller. It reads a normalized catalog data as an external file to model the absorption chiller. TRNSYS software provides the mathematical reference of how to make the normalized catalog data of the chiller being simulated. The normalized catalog data consists of four input variables: chilled water set point, t_{Eo} in this case, entering cooling water temperature to the absorber (t_{Ai}), inlet hot water temperature to the desorber (t_{Di}), and fraction design load ($f_{Design\ Load}$). The fraction design load is a fraction of the design capacity at which the absorption chiller is currently operating. The fraction design load is defined as:

$$f_{Design\ Load} = \frac{\dot{Q}_{removed}}{\dot{Q}_{E,nominal}} \tag{3.1}$$

The output variables of the external data are the fraction capacity ($f_{capacity}$) and the fraction of design energy input ($f_{Design\ Energy\ Input}$). The fraction capacity is then expressed as follows:

$$f_{capacity} = \frac{\dot{Q}_E}{\dot{Q}_{E,nominal}} \tag{3.2}$$

where $\dot{Q}_E$ is capacity at particular t_{Ai}, t_{Eo}, and t_{Di} at which the absorption chiller is currently operating. While the fraction design energy input is calculated as:

$$f_{Design\,Energy\,Input} = \frac{f_{Design\,Load} \cdot \dot{Q}_D}{f_{capacity} \cdot \dot{Q}_{D,nominal}} \tag{3.3}$$

where $\dot{Q}_{D,nominal}$ is a nominal driving heat, and $\dot{Q}_D$ is a driving heat at particular t_{Ai}, t_{Eo}, and t_{Di} at which the absorption chiller is currently operating.

To make an external file for the absorption chiller (i.e. type BEE – 50 kW), first, $\dot{Q}_D$ and $\dot{Q}_E$ are calculated using the characteristic equation of the absorption chiller that has been presented in chapter 2 with the variation range of t_{Ai} from 20°C to 40°C with an interval of 5°C, t_{Eo} from 6°C to 16°C with an interval of 2°C, and t_{Di} from 75°C to 90°C with an interval of 5°C. Then, $f_{capacity}$ can be obtained. Afterward, with the variation of $f_{Design\,Load}$ from 0 to 1 with an interval of 0.1, $f_{Design\,Energy\,Input}$ can also be obtained. This calculation is performed using the EES software as can be seen in Appendix 1. Then, these results are used as an external file in the simulation carried out using TRNSYS (as can be seen in Appendix 2). With this external file, type 107 represents the performance of the absorption chiller BEE – 50 kW.

- Heat Exchanger 1 (HX-1) – Calculator

  The calculator used for Heat Exchanger 1 is to calculate the potential Domestic Hot Water that can be produced. The equation is:

$$\dot{Q}_{DHW} = \dot{m}_h \cdot cp_{water} \cdot \Delta T_h \tag{3.4}$$

where $\dot{Q}_{DHW}$ is the potential domestic hot water capacity in kW, $\dot{m}_h$ is the mass flow of the hot side of the heat exchanger 1, that is, district heating line that leaving the desorber in kg/s. Cp_{water} is the specific heat capacity of water (taken as 4.19 kJ/kg·K) and ΔT_h is the temperature difference between inlet and outlet of the heat exchanger 1 of the hot side. Thus, the potential domestic hot water production can be calculated as:

$$\dot{V}_{DHW} = \frac{\dot{Q}_{DHW} * 3600}{\rho_{water} \cdot cp_{water} \cdot (T_{sp,DHW} - T_{mains})} \tag{3.5}$$

where $\dot{V}_{DHW}$ is the domestic hot water flow potential in m^3/h, ρ_{water} is the density of water, $T_{sp,DHW}$ is the set point domestic hot water temperature of 60°C, and T_{mains} is the water temperature from the mains stream (municipality stream). The domestic hot water production follows the operational time of the absorption machine in both heating and cooling mode of operation.

3.3.1 Cooling Mode Simulation

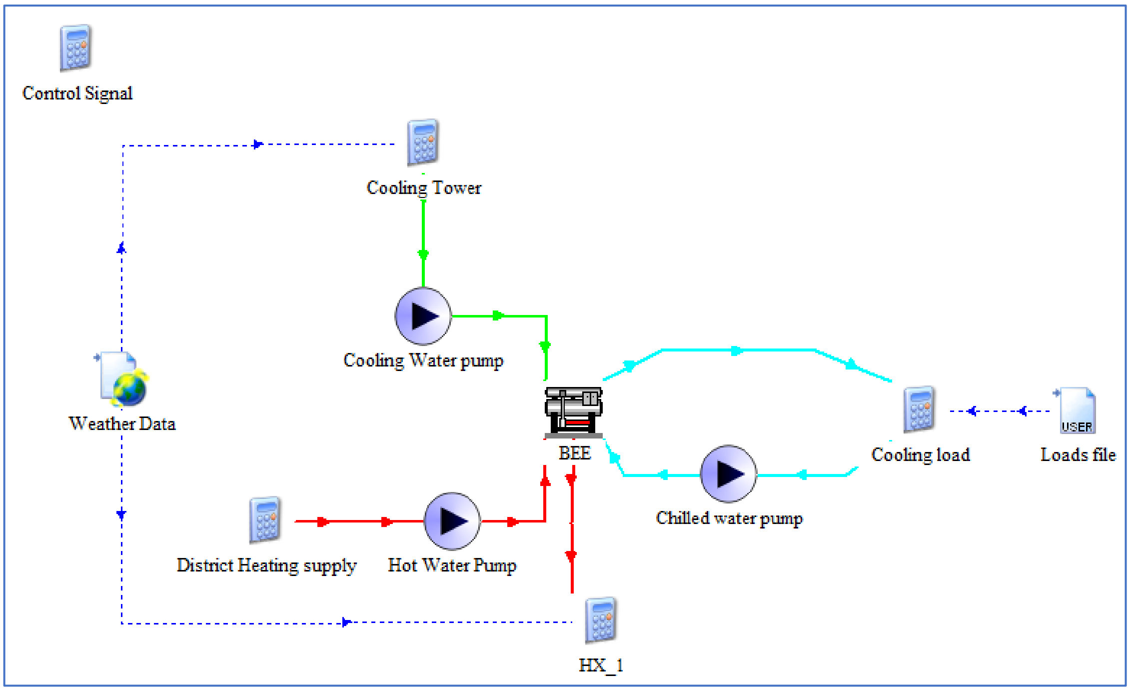

Figure 3.11. TRNSYS layout for cooling mode simulation

In the cooling mode simulation (Figure 3.11), the additional components are the control signal of the system and a dry cooler. Both components are represented by a calculator since the interesting information for the dry cooler is only the absorber's external stream inlet temperature and the control signal can be done by the calculator. For the dry cooler, the inlet temperature of the absorber external stream is assumed to have a temperature of 2 K higher than the ambient dry bulb temperature (Kühn *et al.*, 2010). On the other hand, as it is already explained in the system description, this temperature (t_{Ai}) cannot be lower than the minimum allowed temperature by the absorption chiller, in this case, it is 20°C. Thus, the equation for the absorber external stream inlet temperature representing as dry cooler outlet is:

$$t_{Ai,min} = max(20, t_{db} + 2) \tag{3.6}$$

where t_{db} is air dry bulb temperature at current condition when the absorption chiller is operating. However, with this equation, it is possible that the cooling capacity is lower than the load when the absorber external stream inlet temperature is higher than the required absorber's external stream inlet temperature to produce the cooling capacity. To avoid this issue, the absorber inlet temperature can be limited with the required absorber inlet temperature at maximum cooling demand. Since t_{Di} and t_{Eo} are fixed, then, t_{Ai} for maximum cooling demand can be calculated from the characteristic equation. Thus, the equation becomes:

$$t_{Ai,max} = max\left(20, \min\left(t_{Ai,max}, t_{db} + 2\right)\right) \tag{3.7}$$

, where $t_{Ai,max}$ is the maximum inlet temperature of the absorber's external stream to provide the maximum cooling demand. For the control signal of the absorption chiller, since this simulation is only in cooling mode, then the control signal will turn on the absorption chiller when there is cooling demand (cooling demand > 0). While when there is no cooling demand, the absorption chiller will be off.

3.3.2 Heating Mode Simulation

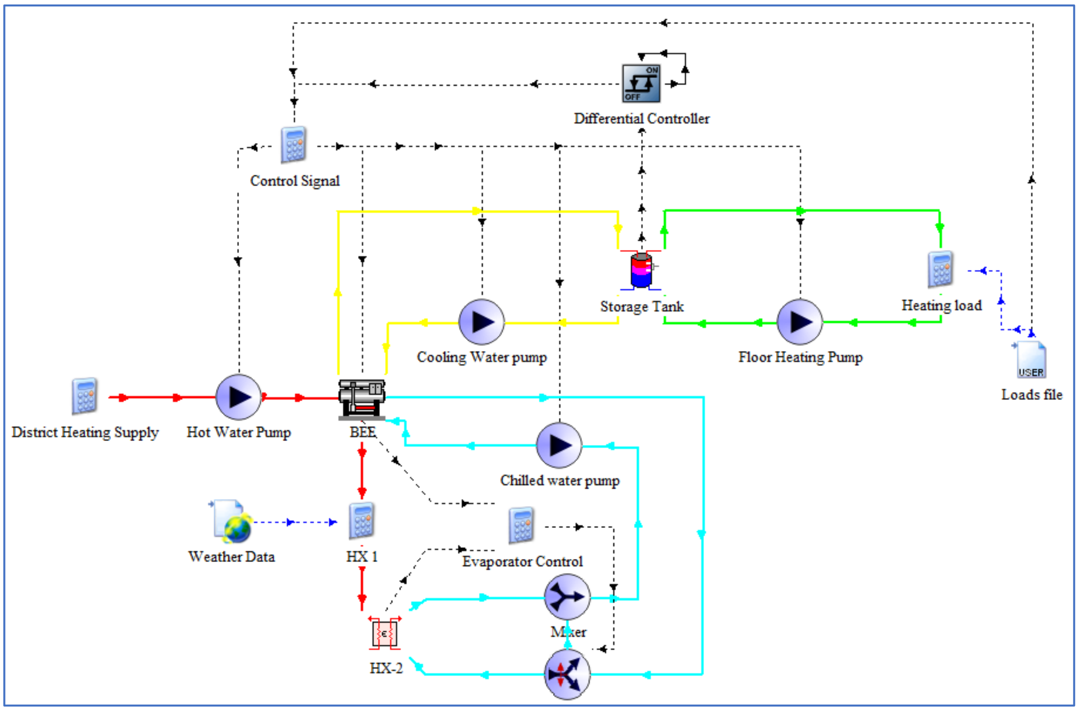

Figure 3.12. TRNSYS layout for heating mode simulation

In heating mode simulation, the additional components are Storage Tank, valve 5, mixer, Heat Exchanger 2, differential controller, and floor heating pump.

- Storage Tank – Type 60c

  As it is mentioned before, the storage tank is only used in a heating mode where it will store the useful heat from the absorption machine (in this case, absorption heat pump). This type requires several parameters such as the volume and height of the tank. The volume of the tank is calculated as follows:

$$V_{tank}(m^3) = \frac{\dot{Q}_{AC,nominal} \cdot n_{hours} \ * 3600}{\rho_{water} \ \cdot \ cp_{water} \cdot \ \Delta T_{tank}} \tag{3.7}$$

  , where ΔT_{tank} (K) is the difference between the minimum and maximum temperature of the floor heating supply temperature. In this case, the floor heating supply temperature operates between 30°C to 40°C (Danfoss, 2010), thus ΔT_{tank} is 10 K. $\dot{Q}_{AC,nominal}$ is the nominal heat produced by the absorption heat pump, and n_{hours} is the time stored parameter, where it is a number of hours needed to operate the absorption chiller to store the energy in the tank. In this case, time stored parameter is calculated as the ratio between average daily heating demand and the nominal heat produced by the absorption heat pump. In other words, the time stored parameter is the number of hours where the absorption heat pump stores the nominal energy in the storage tank to supply average heating demand for a day. Thus, the time stored parameter is expressed as:

$$n_{hours} \ (h) = \frac{Daily \ Average \ Heating \ Demand \ (kWh)}{\dot{Q}_{AC,nominal}(kW)} \tag{3.7}$$

  Daily average heating demand is calculated from the annual heating demand divided by the number of hours of the heating demand. After time stored parameter is calculated, the volume of the tank can be obtained. Now, to obtain the height of the tank, it is assumed that the ratio between the height and diameter of the tank is 2. Thus, the height of the tank is calculated as:

$$h_{tank} \ (m) = \left(\frac{4 \cdot V_{tank} \cdot 2^2}{\pi} \right)^{\frac{1}{3}} \tag{3.8}$$

  , where h_{tank} is the height of the tank. The last part is to determine the heat loss coefficient of the tank. In this case, the tank is assumed to have a typical insulation using Polyurethane with the conductivity coefficient of 0.0260 W/m·K with the thickness of 5 cm (Fantucci *et al.*, 2015).

- Valve 5 – Type 11f

  Type 11f is a diverter that is used to divert the flow from the outlet of the evaporator. Part of the flow will go to the flow leaving HX-2 in case that the outlet temperature of HX-2 is higher than the maximum allowable temperature, that is, 21°C.
- Heat Exchanger 2 – type 91

  Type 91 is a constant effectiveness heat exchanger model. In this case, a typical effectiveness value of the heat exchanger is considered (i.e., 0.9) since it is a water-water heat exchanger. Since this heat exchanger is to transfer heat to the evaporator external circuit/loop during heating mode as a heat source, the minimum temperature of the inlet of heat exchanger 2 from the district heating line can be calculated using the following expression:

  $$\varepsilon = \frac{(\dot{m} \cdot Cp_{water})_c \cdot (T_{c,out} - T_{c,in})}{(\dot{m} \cdot Cp_{water})_h \cdot (T_{h,in} - T_{c,in})} \tag{3.9}$$

  , where ε is the effectiveness of heat exchanger 2, $(\dot{m} \cdot Cp_{water})_c$ is the heat capacity of the cold side, that is, the evaporator external stream. $T_{c,out}$ is the design maximum inlet evaporator temperature of 21°C, $T_{C,in}$ is the set point outlet evaporator temperature of 16°C, $(\dot{m} \cdot Cp_{water})_h$ is the heat capacity of the district heating that enters the heat exchanger 2, and $T_{h,in}$ is the minimum temperature of the inlet of heat exchanger 2 from district heating line. In the equation, the heat capacity of district heating that enters heat exchanger 2 is the minimum heat capacity because the district heating flow is lower than the evaporator circuit flow. Thus, since all variables are known, then the minimum temperature of the inlet of heat exchanger 2 can be found. It is around 31°C. Below this temperature, the heat exchanger cannot increase the temperature of the evaporator circuit to 21°C if the inlet is 16°C.
- Differential controller – Type 2b

  This type is used as an on/off controller. It is a controller that generates a signal as a function of the difference between upper and lower temperature input. In this case, this differential controller is used to control the signal of the absorption heat pump. Since the supply temperature of the heating floor is 30°C to 40°C, then the absorption heat pump is controlled according to this temperature. The absorption heat pump will on when the supply temperature of the heating floor is 30°C, while the absorption heat pump will off when the supply temperature of the heating floor reaches 40°C.

- Floor Heating Pump – Type 114

  The floor heating pump is a circulation pump for the building's floor heating. It uses a single speed pump. The mass flow rate of the pump is calculated as:

$$\dot{m}_{floorHeating}\left(\frac{kg}{s}\right) = \frac{Heating\ Load_{max}\ (kW)}{Cp_{water}\left(\frac{kJ}{kg \cdot K}\right)\left(T_{supply} - T_{return}\right)\ (K)} \tag{3.10}$$

  , where $\dot{m}_{floorHeating}$ is the mass flow of floor heating pump, $Heating\ Load_{max}$ is the maximum heating load of the building, T_{supply} is the supply temperature and T_{return} is the return temperature. In floor heating system, a maximum temperature difference between supply and return temperatures is 5 K (Kühn, Özgür-Popanda and Ziegler, 2010). Thus, in a single-speed pump, this temperature difference corresponds to the maximum heating load. Hence, the lower heating load will have a temperature difference lower than 5 K. This pump is controlled based on the heating load. This pump is on when there is heating load (Heating Load > 0) and it will be off when there is no heating load.

3.3.3 Performance Indicator

The performance indicator for the proposed system is the seasonal COP during heating mode and cooling mode (given by Eqs. 3.11 and 3.12, respectively). It is a ratio between useful energy produced during the heating and cooling season to the thermal energy supplied in the desorber of the absorption heat pump.

$$COP_H = \frac{Q_H}{Q_D} \tag{3.11}$$

$$COP_C = \frac{Q_c}{Q_D} \tag{3.12}$$

Moreover, the annual primary energy ratio (*PER*) of the system is also carried out. It is a ratio between the sum of useful energy outputs and the primary energy consumed (Noro and Lazzarin, 2020). In this case, the useful outputs are the heating and cooling energies delivered by the absorption heat pump. Since the proposed system is used to cover the space cooling and heating demand as well as potential domestic hot water production, accordingly, the expression for the *PER* becomes:

$$PER_{system} = \frac{Q_C + Q_H + Q_{DHW}}{f_{P,dh} \cdot Q_{dh} + f_{P,el} \cdot \left(\frac{Q_H}{COP_{el,H}} + \frac{Q_C}{COP_{el,C}}\right)} \tag{3.13}$$

where PER_{system} is the primary energy ratio of the system, $f_{P,dh}$ is the district heating primary energy factor in kWh_{prim}/kWh_{th}, Q_{DH} is the energy demand of the system from the district heating network in kWh_{th}, $f_{P,el}$ is electricity primary energy factor in kWh_{prim}/kWh_{el}, $COP_{el,H}$ is the electrical *COP* of absorption heat pump in the heating mode, and $COP_{el,C}$ is an electrical COP of the absorption heat pump in cooling mode. The energy demand of the system from the district heating is thermal energy supplied to the desorber to produce space cooling and heating and to the HX-1 for domestic hot water production. A typical value of non-renewable primary energy factor for district heating is considered as 0.8 in the European Union (Euroheat & Power, 2011), while the electricity primary energy factor is 2.06. The electricity primary energy factor corresponds to non-renewable primary energy factor of the electricity generation mix in the European Union (Fritsche and Greß, 2015). For electricity consumed by the absorption heat pump, a constant electrical COP is considered. It is reported that the electrical COP of this absorption heat pump is 20 kW_{th}/kW_{el} in cooling mode by considering the electricity consumed for heat rejection devices and pumps at nominal flow rates (Güido *et al.*, 2018). Consequently, this value is used in the proposed system performance analysis.

The performance comparison between the proposed system and a conventional (reference) system is also carried out in this investigation. The overall schematic of the proposed system and reference system for comparison purposes are depicted in Figure 3.13 and Figure 3.14, respectively. The reference system is using a boiler to produce heat for domestic hot water production and space heating application. While in summer, it uses a vapor compression chiller to cover the space cooling demand.

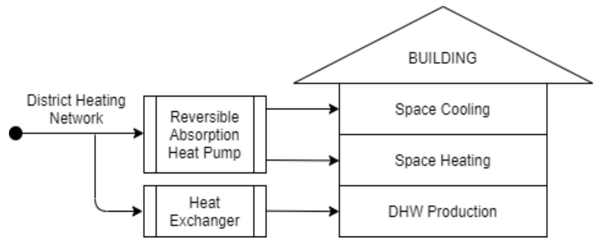

Figure 3.13. Proposed System configuration for performance comparison

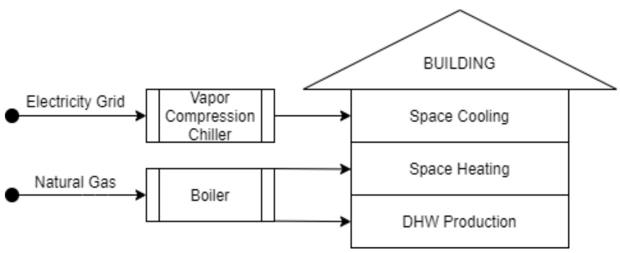

Figure 3.14. Reference System configuration for performance comparison

In this case, the comparison is calculated from the primary energy ratio and primary energy saving of the proposed system. The reference system is used to cover the same space cooling and heating demand, and to produce the same amount of energy for domestic hot water production. The primary energy ratio for the conventional system is calculated as:

$$PER_{ref} = \frac{Q_H + Q_C + Q_{DHW}}{f_{P,Heat-Boiler} \cdot (Q_H + Q_{DHW}) + f_{P,el} \cdot \left(\frac{Q_C}{COP_{VCC}}\right)} \tag{3.14}$$

where PER_{ref} is the primary energy ratio of the reference system, $f_{P,Heat-Boiler}$ is the primary energy factor for boiler to produce heat utilizing natural gas, a typical value is considered as 1.1 by assuming the boiler efficiency of 0.9. COP_{VCC} is the COP of vapor compression chiller. In this case, the type of vapor compression chiller is considered as air-cooled vapor compression chiller since the building is a small office building. The typical COP of an air-cooled vapor compression chiller is 2.4 at 7°C supply temperature (Yu *et al.*, 2014), however, since this is a chilled ceiling with a supply temperature of 16°C, a typical COP will increase around 20% higher (CBCA, 2012). Thus, COP_{VCC} is considered as 2.88.

The primary energy saving (PES) can be also considered. It is a difference between primary energy required in the proposed system ($PE_{proposed}$) and the primary energy required in the reference system (PE_{ref}). The primary energy required for both systems is calculated from the denominator in the Eqs. 3.13 and 3.14. The equations are:

$$PE_{proposed} = f_{P,dh} \cdot Q_{dh} + f_{P,el} \cdot \left(\frac{Q_H}{COP_{el,H}} + \frac{Q_C}{COP_{el,C}}\right) \tag{3.15}$$

$$PE_{ref} = f_{P,Heat-Boiler} \cdot (Q_H + Q_{DHW}) + f_{P,el} \cdot \left(\frac{Q_C}{COP_{VCC}}\right) \tag{3.16}$$

Thus, the primary energy saving is simply calculated as:

$$PES = PE_{proposed} - PE_{ref} \tag{3.17}$$

However, to clearly see the comparison, it is useful to see the primary energy saving as a percentage with respect to the primary energy of reference system. It is expressed as:

$$\%PES = \frac{PE_{proposed} - PE_{ref}}{PE_{ref}} \cdot 100\% \tag{3.17}$$

4. RESULTS AND DISCUSSION

This chapter aims to show the results of space heating and cooling demand of the selected small office buildings in Berlin and Barcelona. After that, the monthly performance of the absorption machine in reversible operation mode to cover the demand is discussed. Interesting results such as the annual operational time of the system and the potential domestic hot water production are presented. Finally, the annual primary energy ratio and its comparison to the conventional system are shown.

4.1 Space Heating and Cooling Demand

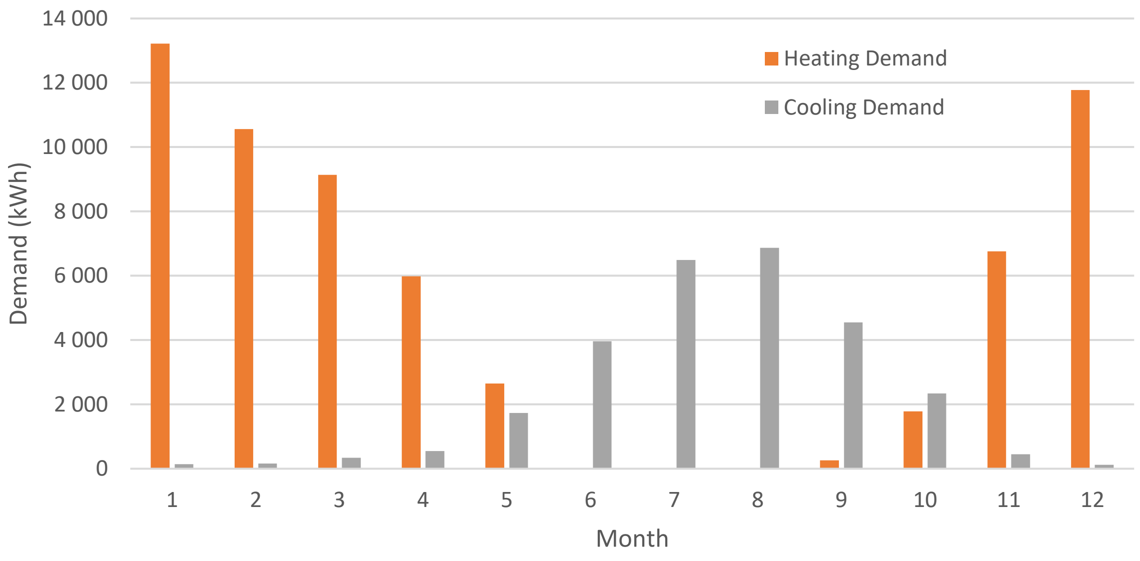

Figure 4.1. Monthly heating and cooling demand in Barcelona

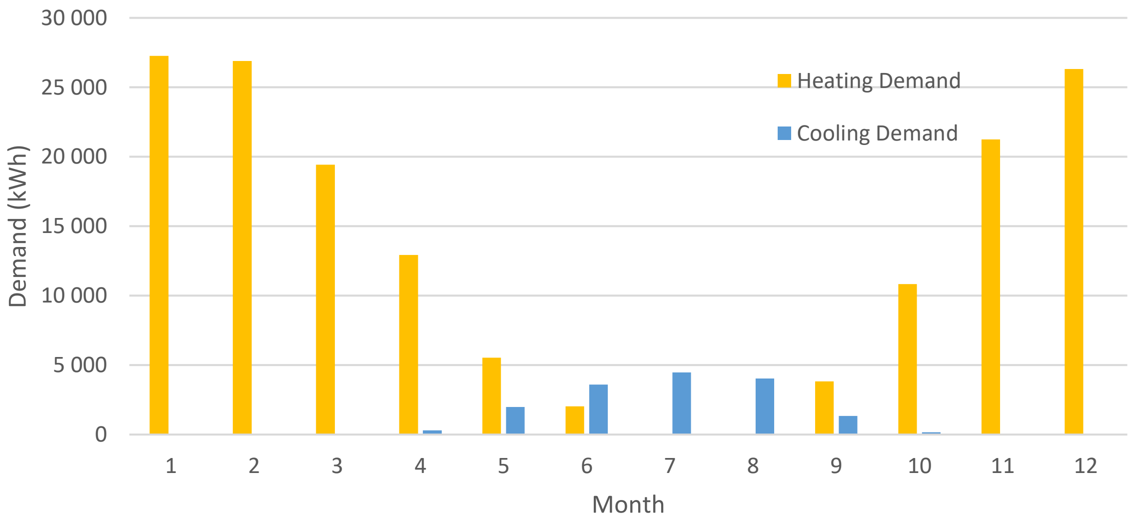

Figure 4.2. Monthly heating and cooling demand in Berlin

As it can be seen in Figures 4.1 and 4.2, the cooling and heating demand of the building varies according to time. In this case, the monthly results show that cooling demand for Berlin only appears from March to October, while in Barcelona the cooling demand is needed throughout the year. The maximum monthly cooling demand for Barcelona is in August with 6868.31 kWh. The peak hourly cooling demand is also in the same month with a value of about 45.15 kW. In Berlin, the maximum monthly cooling demand is lower than in Barcelona, only 4465.29 kWh in June, and the peak hourly cooling demand is 44.39 kW. This small difference in peak cooling demand is because the solar heat gains of Berlin at that time is higher than the solar heat gain in Barcelona. As it can be seen below in Figures 4.3 and 4.4, Berlin has higher solar heat gain in summer compared to the building in Barcelona.

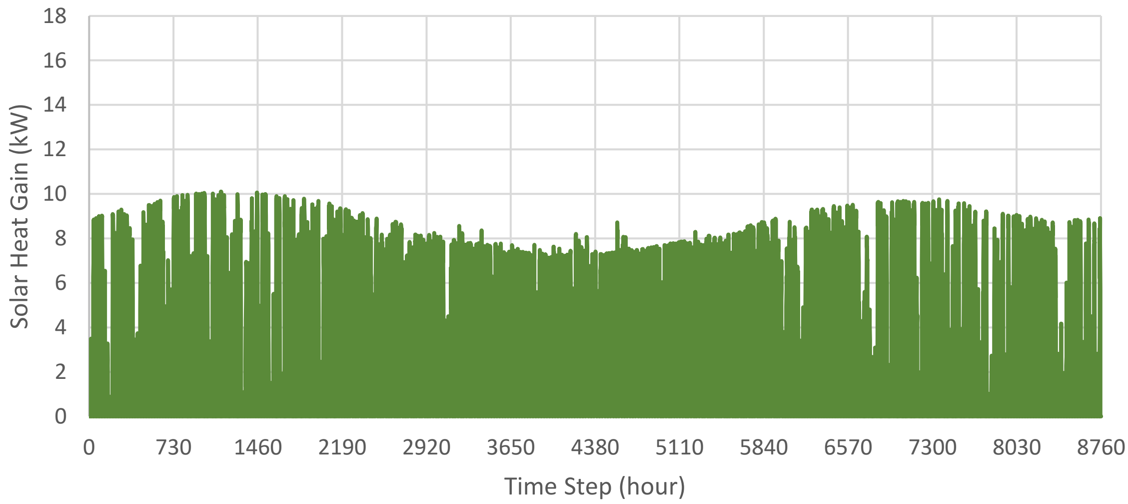

Figure 4.3. Solar Heat Gain of the building in Barcelona

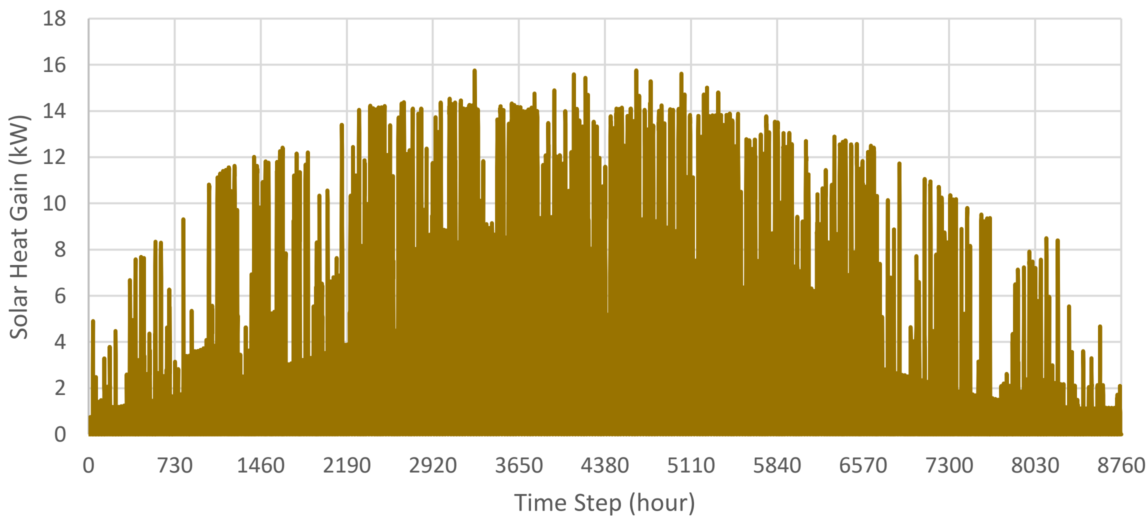

Figure 4.4. Solar Heat Gain of the building in Berlin

The range of daily peak solar heat gain for Barcelona is between 7.5 kW and 10 kW while in Berlin is between 3 kW and 15 kW. This short-range of daily peak solar heat gain in Barcelona shows that there is no significant difference in solar heat gain to the building throughout the year. While a different case in Berlin, that the solar heat gains change significantly where the highest solar heat gain occurs in the summer period. However, the ambient temperature is still higher in Barcelona, thus, the peak cooling demand in Barcelona is a little bit higher. The total cooling hours in Berlin is 1103 hours which accounts for around 12.6% of the year and Barcelona is about 1919 hours which accounts for 21.9% of the year.

For heating demand, the building in Berlin (see Figure 4.2) has a much higher heating demand than in Barcelona (see Figure 4.1). The period where there is no heating demand in Barcelona is longer than in Berlin. Heating is not needed in July and August for Berlin, while in Barcelona is from June to August. The peak heating demand for the building in Barcelona occurs in December with the value of 47.80 kW and Berlin is 75.73 kW in February. This peak heating demand seems very low compared to the absorption heat pump capacity at the nominal condition, which is 113 kW. This is the reason why the hot storage tank is used in the present study. The total heating hours in Berlin is around 5958 hours which accounts for 68% of the year and Barcelona is around 4237 hours which accounts for 48.4% of the year.

4.2 Performance of the Absorption Machine during Heating Mode

The performance of the absorption machine during the heating mode can be seen in Figure 4.5. In heating mode, Barcelona has a higher heating COP_H than Berlin. This is because the district heating temperature of Barcelona is higher than Berlin, where Barcelona is 90°C and Berlin is 80°C. Another interesting result can be seen in Figure 4.6 where it is an average inlet temperature of the absorber's external stream during heating mode. The absorber inlet temperature for Barcelona is always lower than Berlin throughout the year. This is representing that the COP_H of Barcelona is higher than in Berlin. However, it can be seen also that the COP_H is getting lower every month from January until the last month before there is no heating demand. This is because the demand is getting lower every month, and since the system works at a single-speed pump, it means the mass flow does not change. This condition makes the return temperature to the inlet of the absorber is getting higher. It can be seen in Figure 4.6 that the average inlet temperature is higher every month. Hence, since the inlet of absorber temperature is higher, the COP_H is lower.

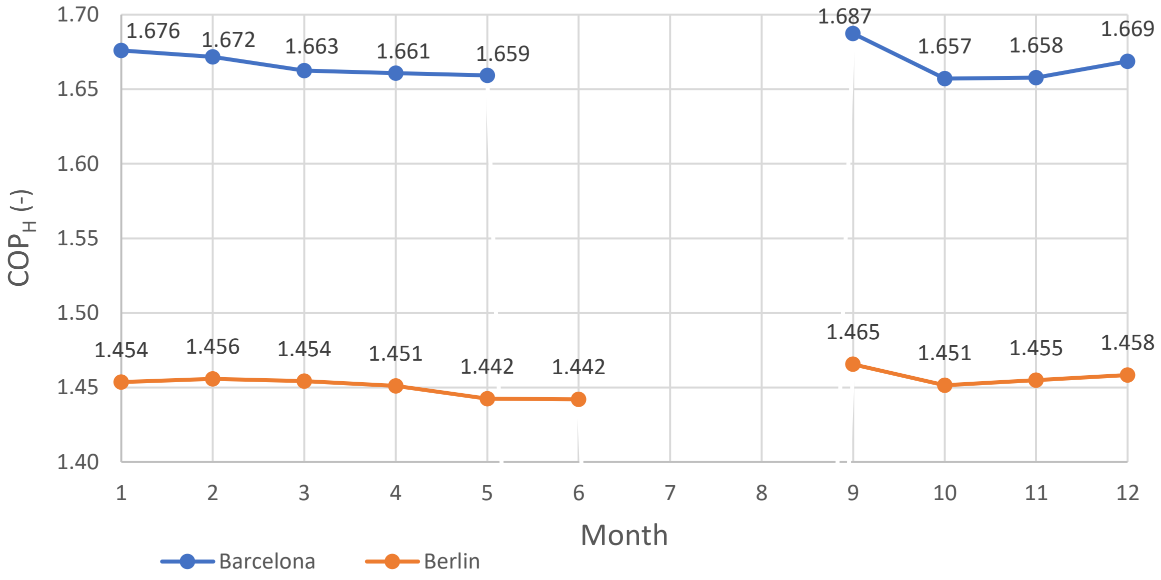

Figure 4.5. Seasonal Heating COP of the absorption machine

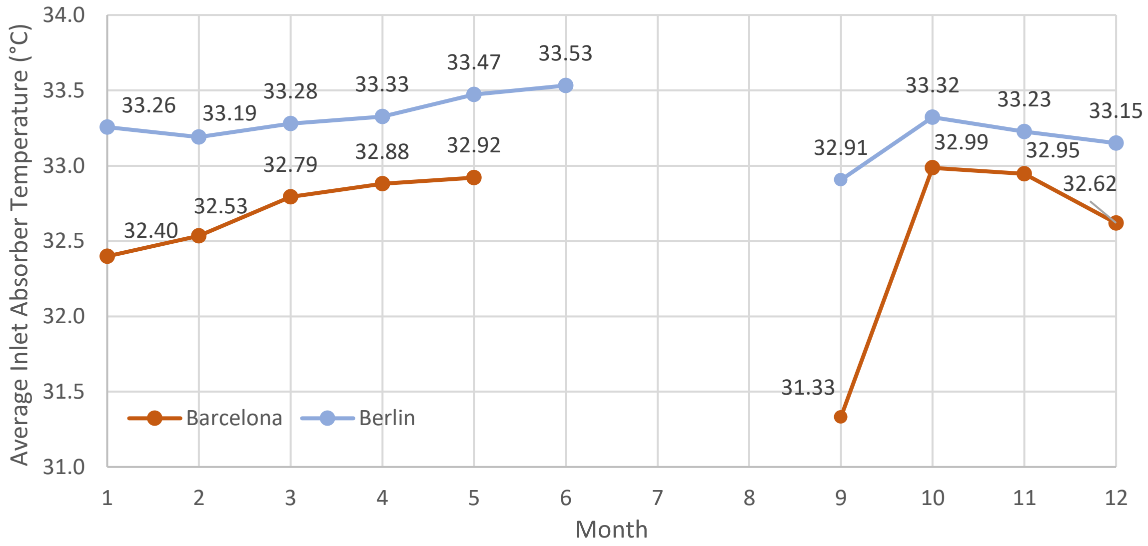

Figure 4.6. Average Inlet Temperature of Absorber external stream during heating mode

During the summer period where there is no heating demand, the hot water storage tank is not used. Because of that, the temperature in the storage tank decreases over time due to the heat losses of the tank. As a result, in October, where the heating mode is back in operation, the absorber inlet temperature is lower than usual. In consequence, since the absorber inlet temperature is lower, then the COP_H will be higher. It can be seen in Figure 4.5 that the highest COP_H values occur this month where it is 1.687 for Barcelona, and 1.465 for Berlin. The annual COP_H for the system in Berlin is 1.454 and for Barcelona is 1.667.

4.3 Performance of the Absorption Machine during Cooling Mode

In cooling mode, the absorption machine in Barcelona operates throughout the year since the cooling demand appears throughout the year. While in Berlin, it is only from March to October. The seasonal COP (COP_C) of the absorption machine is depicted in Figure 4.7. Since the district heating temperature is assumed constant all over the year, and the chilled water supply temperature is maintained always at 16°C, thus, the capacity of the absorption machine depends on the cooling tower outlet temperature. As it is explained in chapter 3 that the cooling tower outlet temperature is limited to a required temperature for the maximum cooling demand. This has to be done because, if the outlet cooling tower temperature is higher than the required temperature to supply the demand, then the absorption machine cannot supply the demand, thus, the setpoint temperature will not be satisfied. For this condition, the maximum outlet temperature for Berlin is about 28°C which corresponds to the maximum cooling demand of 44.39 kW. While in Barcelona is about 32°C which corresponds to maximum cooling demand of 45.15 kW. With this condition, it means that the inlet temperature of the absorber's external stream for the system in Barcelona has a longer range than in Berlin. It makes the monthly average absorber inlet temperature of Berlin is lower than Barcelona as illustrated in Figure 4.8.

The COP_C of the absorption machine is going lower by the time the absorber's external stream inlet temperature is getting higher. The COP_C seems higher than the nominal COP (i.e., $COP_{C,\ nominal}$ = 0.79) because the inlet temperature of the absorber's external stream is lower than its nominal value (i.e., 30°C). In January and February, the COP_C is higher in February than in January because the absorber inlet temperature in February is also lower. The interesting condition happens in May to October where the COP_C of Berlin is lower from May to June while the rest is higher than COP_C of Barcelona. From May to June, the difference in the absorber external stream inlet temperature between the system in Berlin and Barcelona is not so high, it is lower than 1°C, with the district heating temperature that higher in Barcelona, this condition makes the COP_C in Barcelona is higher than in Berlin. However, from July to October, the difference in absorber's external stream inlet temperature is even higher than 2°C. Since the absorber external stream inlet temperature in Berlin is much lower, the COP_C in Berlin is higher. As it is mentioned, the absorber external stream inlet temperature is the cooling tower outlet temperature, which depends on the ambient condition and is limited to a temperature that corresponds to the maximum cooling load.

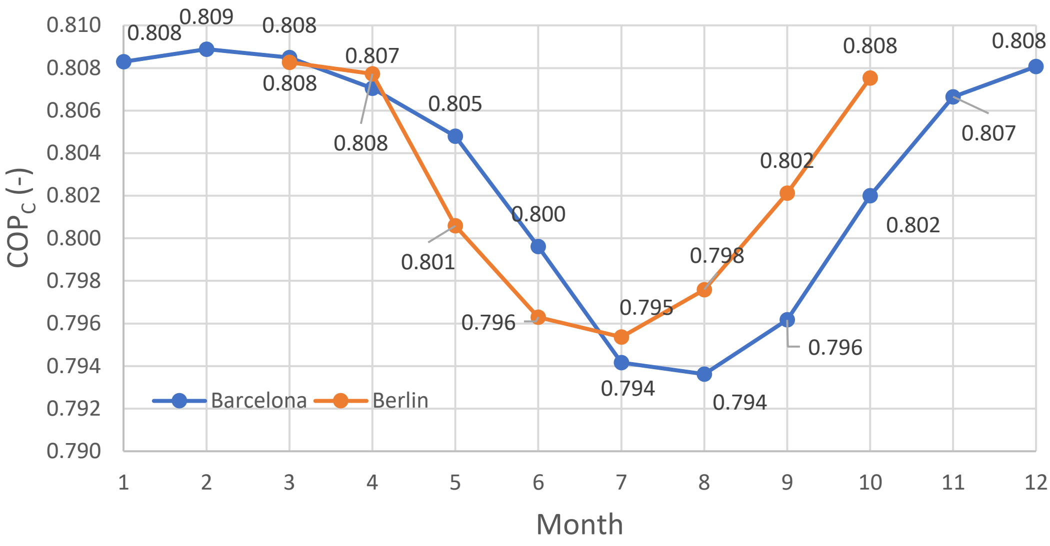

Figure 4.7. Seasonal Cooling COP of the absorption machine

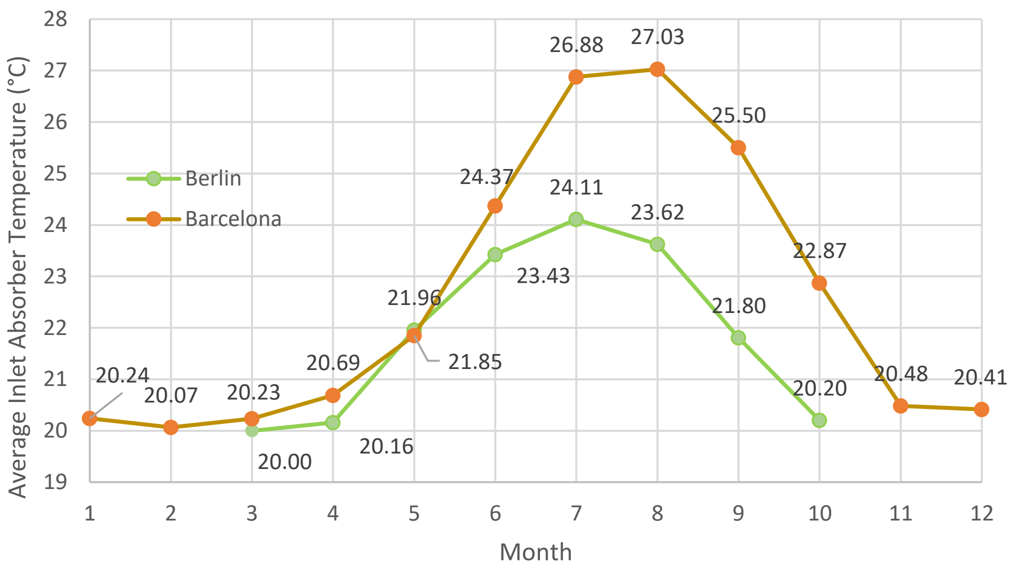

Figure 4.8. Average Inlet Temperature of Absorber external stream during cooling mode

4.4 Annual Operational Time of The Reversible Absorption Machine

It is useful to see the operational time of the system since the absorption machine works as a reversible operation. In cooling mode, the absorption machine operates according to when the cooling demand appears. It means that the operational hours of the absorption machine in cooling mode are the same as the cooling hours, that is, about 21.9% of the year for Barcelona and 12.6% of the year for Berlin (Figures 4.9 and 4.10, respectively).

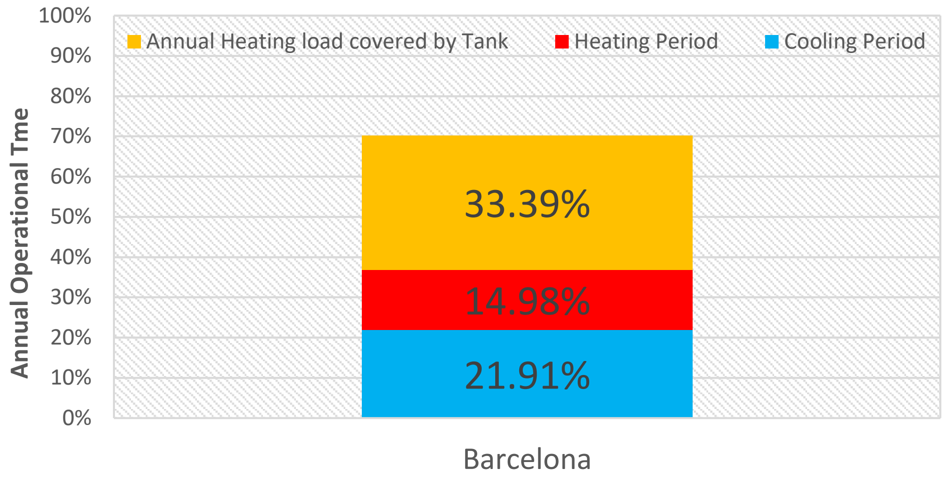

Figure 4.9. Annual operational time in Barcelona

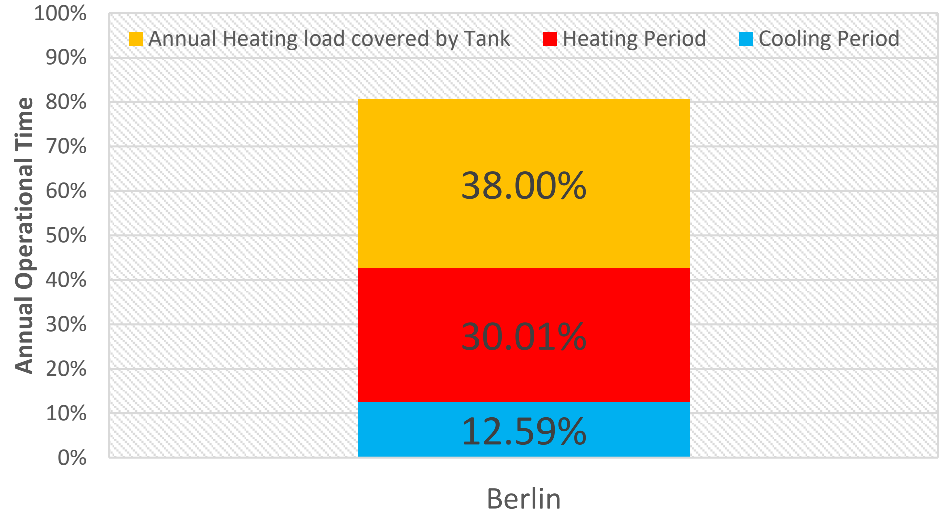

Figure 4.10. Annual Operational Time in Berlin

From the result of heating demand, the daily average heating demand that should be supplied can be determined. It is 352.09 kWh/day in Barcelona and 629.84 kWh/day in Berlin. These values lead to a bigger tank for the building in Berlin since the tank is sized to store the daily average heating demand. As a result, the absorption machine works more time in Berlin to store the energy in the tank so the tank can cover the heating demand. It can be seen in Figures 4.9 and 4.10 that the operational time for absorption machine in heating mode is only around 15.0% of the year for Barcelona and 30.0% of the year for Berlin. It seems the operational time for Berlin is almost doubled and it corresponds to the daily average heating demand that also almost doubled. The absorption machine works only when there is a heating demand and when the temperature inside the tank is lower than the minimum permissible supply temperature of the heating floor (30°C). When the temperature of the tank reaches the maximum permissible supply temperature (40°C), the absorption machine will off. Then, the demand will be covered by the tank as long as the temperature of the tank is between 30°C to 40°C. This period accounts for about 33.4% of the year in Barcelona and 38% of the year in Berlin. In other words, these values also correspond to the number of heating hours when the absorption machine is off.

From these results, it can be seen that if the absorption machine only works as an absorption chiller, it only operates for about 21.9% of the year in Barcelona, even worse in Berlin. But with this reversible system, the absorption machine can work for a longer period.

4.5 Potential Domestic Hot Water Production

Potential domestic hot water production is calculated from the maximum heat that can be transferred from the district heating line leaving the desorber of the absorption machine to increase the municipal water temperature to 60°C. The maximum heat that can be transferred is determined by the difference of desorber's external stream outlet temperature and the minimum temperature entering heat exchanger 2 (Figure 3.14). In this result, the monthly average volumetric flow rate of potential domestic hot water production in cooling mode and heating mode are presented in Figure 4.11. It can be seen in Figure 4.11 that in cooling mode, the system in Barcelona produces more domestic hot water than in Berlin. This is because the operational time of the absorption machine in cooling mode is higher in Barcelona than in Berlin. The same case for domestic hot water production in heating mode, the production in Berlin is higher because the operational time of the absorption machine in heating mode is higher in Berlin than in Barcelona. However, in both cities, domestic hot water production in cooling mode is higher than in heating mode. This is because the outlet desorber temperature in cooling mode is higher.

Figure 4.12 shows the frequency of the desorber external stream outlet temperature. It can be seen that in heating mode, the outlet temperature of the desorber in Barcelona is only in the range of 72°C to 74°C, while in Berlin it is between 60°C and 64°C. This is because the absorption machine works in full capacity to cover the storage tank. In cooling mode, the outlet desorber temperature depends on the demand since the flow rate is constant. Mostly, the demand is lower than the capacity of the machine, thus the desorber outlet temperature is quite high. Since the overall desorber outlet temperature is higher in cooling mode, thus the potential heat for domestic hot water production is higher. As a result, the volumetric flow rate of domestic hot water is also higher in cooling mode. Moreover, the maximum potential domestic hot water is produced in the month where the cooling demand is also maximum, June for Berlin and August for Barcelona with the value of 1.23 m^3/h and 2.22 m^3/h, respectively.

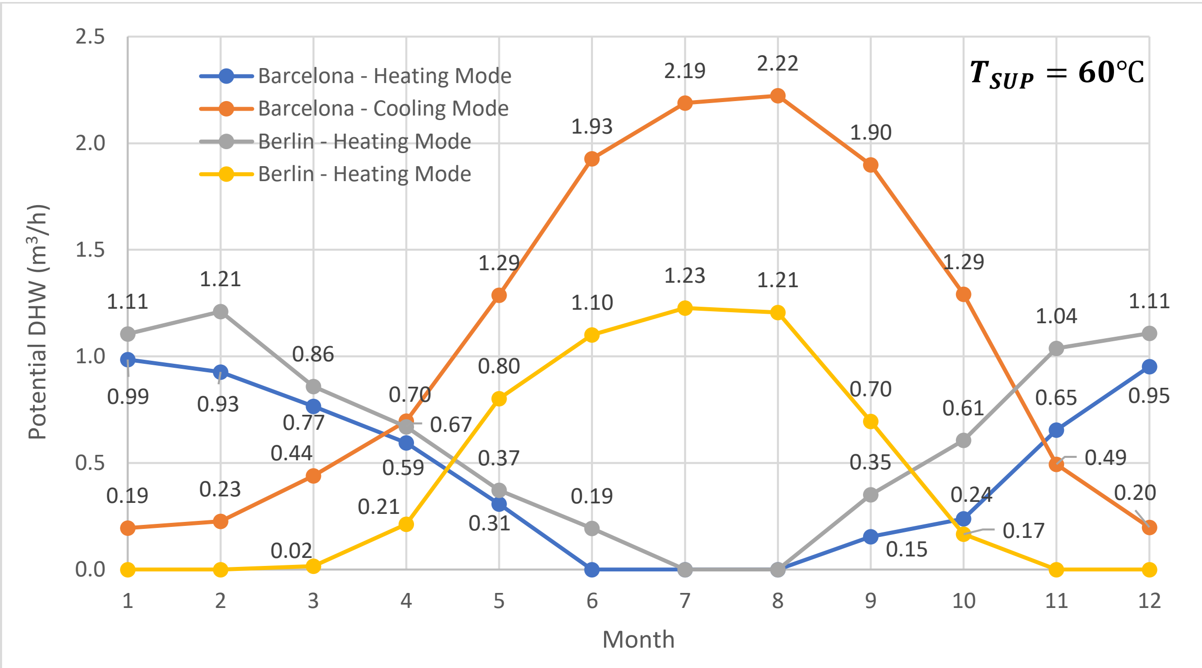

Figure 4.11. Potential Domestic Hot Water Volumetric Flow Rate

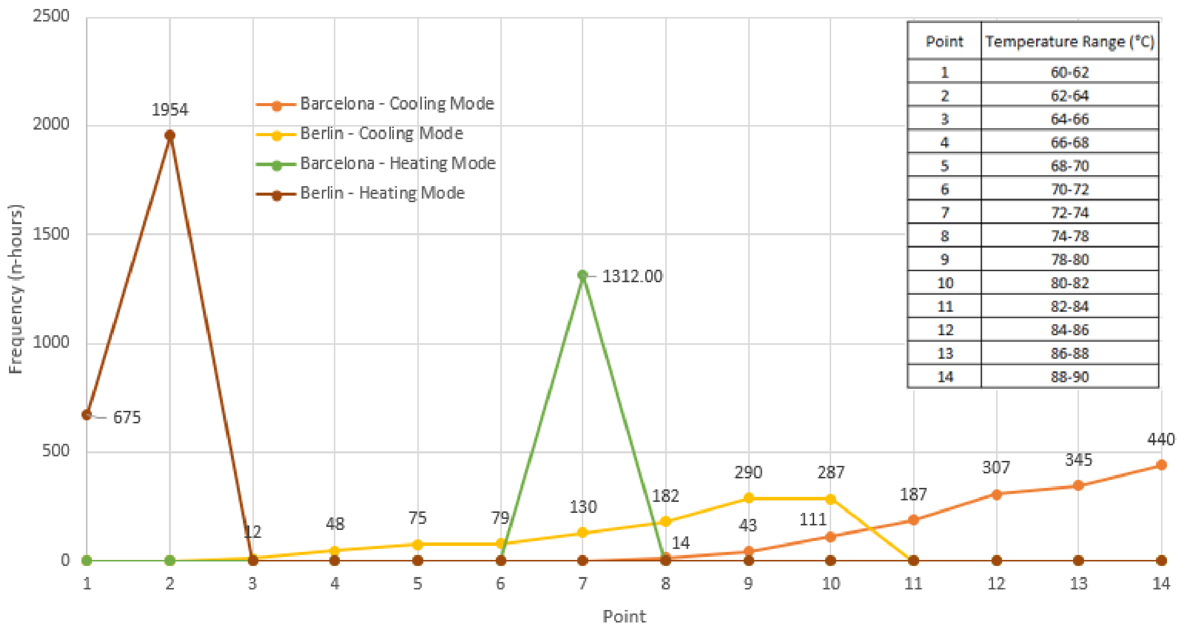

Figure 4.12. Frequency of Desorber external stream Outlet Temperature

4.6 Primary Energy Ratio and Comparison to the Reference System

The useful energy outputs provided by the system are space heating, space cooling, and domestic hot water. In this case, the annual PER is analysed (Figures 4.13 and 4.14). For the system in Barcelona, it is used to cover annual space heating of 62138.74 kWh, annual space cooling of 27702.65 kWh, and annual potential domestic hot water of 650200.34 kWh. It can be seen in Figure 4.13 that the primary energy ratio for the proposed system is around 1.27, which means that the useful energy produced is higher than the fuel consumed. For space heating, the energy consumed from the district heating is only 37272.92 kWh since the annual COP_H for the system in Barcelona is 1.667. Thus, this system seems beneficial compared to an auxiliary boiler that has 90% efficiency. Moreover, the primary energy ratio of the reference system in Barcelona is 0.921 which is lower than the proposed system.

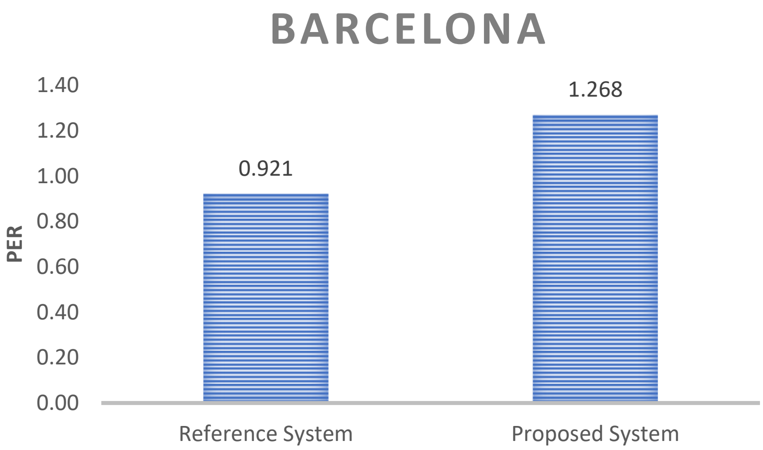

Figure 4.13. PER of Proposed Systems and Reference Systems in Barcelona

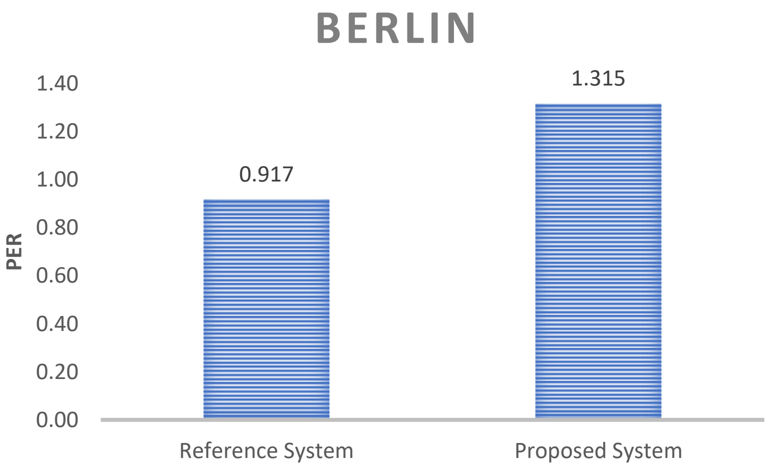

Figure 4.14. PER of Proposed Systems and Reference Systems in Berlin

This is because the primary energy factor for district heating is lower than the primary energy factor of auxiliary boiler to generate heat from natural gas, which are 0.8 and 1.1 respectively. The primary energy factor of district heating is lower because it comes from district heating plant which CHP plant has a big contribution in heat generated for the district heating in European Union as it is explained in chapter 2. In CHP Plant, the primary energy factor for district heating is a result of total primary energy consumed that is subtracted by the total primary energy consumed to generate the electricity (López-Villada *et al.*, 2009), it is the reason that the values are lower than 1.

In the same case for the system in Berlin, it can be seen in Figure 4.14 that the primary energy ratio of the proposed system is 1.315 while the reference system is 0.917. In cooling mode, it is obvious that the vapor compression chiller has higher COP, thus it consumes less energy input. However, since the operational time of the cooling mode is lower than the heating mode, this lower energy consumed is still not enough to make the reference system is better in the annual primary energy ratio assessment.

Table 4.1. Primary Energy Saving of the proposed System

Indicator	Barcelona	Berlin
$PE_{proposed}$ (kWh)	583460.21	521666.71
PE_{ref} (kWh)	803388.07	748401.33
PES (kWh)	219927.86	226734.62
%PES	27%	30%

Since both proposed systems and reference systems use non-renewable primary energy and the results show that the proposed system has a higher primary energy ratio, the primary energy saving can be obtained. It can be seen in Table 4.1 that the proposed system can save 27% of primary energy while in Berlin is 30%. This result proves that the proposed system can reduce fuel consumption, which is beneficial for the environment, the end-user, and also the district heating provider.

5. CONCLUSIONS

In this master thesis, the possibility of using a reversible absorption heat pump at the district heating network substation is carried out where the district heating network supplies driving heat for the absorption heat pump to provide space cooling and space heating applications for a small office building. The potential domestic hot water production using the returning district heating network stream is also analyzed.

A small office building in Barcelona and Berlin is considered to estimate the heating and cooling demand by using the degree-days method. The results clearly show that the Building in Berlin needs more heating than in Barcelona, while cooling is more required in Barcelona. The dynamic performance simulation (carried out in TRNSYS) is used to apply the system to cover these cooling and heating demands as well as the potential domestic hot water production. The system is designed to fit with the demand such as the use of a hot storage tank for heating mode operation and the set of maximum and minimum dry cooler outlet temperature for cooling mode operation.

The system performance simulation shows that the heating COP for the system in Barcelona is higher than in Berlin. This is because the design district heating network supply temperature and absorber cooling water inlet temperature in Barcelona are higher. In cooling mode, there are some months where the cooling COP in Berlin is higher than in Barcelona because absorber cooling water inlet temperature in Berlin is lower. From these results, it can be concluded that the performance of the reversible absorption heat pump in this system depends highly on the absorber cooling water inlet temperature.

In both cities, the potential domestic hot water production in heating mode is lower than cooling mode because the desorber’s hot water outlet temperature in cooling mode is higher, thus the domestic hot water that can be produced is also higher.

The advantage of using this system can be seen from the increase in operational time of the machine. Moreover, the reduction of non-renewable fuel consumption (which is 30% less in Berlin and 27% less in Barcelona) compared to a conventional system. Thus, this system is beneficial for the end-user, district heating provider, as well as for the environment.

REFERENCES

Albers, J. and Ziegler, F. (2016) 'Control Strategies for Absorption Chillers in Chpc-Plants Ensuring Low Hot Water Return Temperatures', in *Heat and Powered Cycles Conference 2016*, pp. 32–37.

Asfand, F. *et al.* (2020) 'Thermodynamic performance and water consumption of hybrid cooling system configurations for concentrated solar power plants', *Sustainability (Switzerland)*, 12(11). doi: 10.3390/su12114739.

ASHRAE (2013a) *2013 ASHRAE Handbook - Fundamentals*. Atlanta, GA: American Society of Heating, Refrigerating, and Air-Conditoning Inc.

ASHRAE (2013b) *ANSI/ASHRAE Standards 90.1-2013, Energy Standards for Buildings Except Low-Rise Residential Buildings (I-P Edition)*.

ASHRAE (2017) *2017 ASHRAE Handbook - Fundamentals*. Atlanta, GA: American Society of Heating, Refrigerating, and Air-Conditoning Inc.

ASHRAE (2019) *ANSI/ASHRAE Standards 62.1-2019, Ventilation for Acceptable Air Quality*. Available at: https://ashrae.iwrapper.com/ASHRAE_PREVIEW_ONLY_STANDARDS/STD_62.1_2019 (Accessed: 1 December 2020).

Ayou, D. S. and Coronas, A. (2020) *New developments and progress in absorption chillers for solar cooling applications*, *Applied Sciences (Switzerland)*. doi: 10.3390/app10124073.

Baelz Automatic (2019) 'Baelz-absorpdynamic absorption chillers'. Heilbronn, Germany: W. Baelz & Sohn GmbH & Co.

Baelz Automatic (2020a) *Baelz Automatic - Absorptionskälteanlagen*. Available at: https://www.baelz.de/systeme/kaelte/ (Accessed: 15 November 2020).

Baelz Automatic (2020b) *Baelz Automatic - Typ Biene 50 kW*. Available at: https://www.baelz.de/systeme/kaelte/biene (Accessed: 15 November 2020).

Bertoldi P *et al.* (2018) *Energy Consumption and Energy Efficiency Trends in the EU-28 2000-2015*. JRC report; European Commission. doi: 10.2760/6684.

Bhatnagar, M., Mathur, J. and Garg, V. (2018) 'Determining base temperature for heating and cooling degree-days for India', *Journal of Building Engineering*, 18(January), pp. 270–280. doi: 10.1016/j.jobe.2018.03.020.

BINE (2012) *Cooling with heat - A new generation of compact chillers cools and heats with low-temeprature heat*. Bronn. Available at: http://www.bine.info/fileadmin/content/Presse/Projektinfos_2012/Projekt_07-2012/ProjektInfo_0712_engl_internetx.pdf.

Bruno, J. C. (2020) 'Polygeneration of Energy and Energy Integration [subject code: 20755106]'. Tarragona: Universitat Rovira i Virgili.

Carrillo, A. (2020) 'Characterization and Modelling of Energy Demand in Buildings [subject code: 20755102]'. Tarragona: Universitat Rovira i Virgili.

CBCA (2012) *An Introduction to Chilled Beams and Ceilings*. Version 1. Reading, Berkshire: Federation of Environmental Trade Associations Ltd. Available at: www.waterloo.co.uk.

Cengel, Y. A. and Ghajar, A. J. (2002) 'Heating and Cooling of Buildings', in *Heat Transfer: A Practical Approach*. 2nd edn. McGraw-Hill Higher Education.

Chardon, G., Le Pierrès, N. and Ramousse, J. (2020) 'On the opportunity to integrate absorption heat pumps in substations of district energy networks', *Thermal Science and Engineering Progress*, 20(June), p. 100666. doi: 10.1016/j.tsep.2020.100666.

CIBSE (2006) *Degree-days: Theory and application, TM41:2006, The Chartered Institution of Building Service Engineers (CIBSE).*

Ciulla G, Lo Brano V and Moreci E (2015) 'Degree Days and Building Energy Demand', in *Southern African Solar Energy Conference 2015*. Kruger National Park, South Africa, pp. 65–70.

Çomakli, K., Yüksel, B. and Çomakli, Ö. (2004) 'Evaluation of energy and exergy losses in district heating network', *Applied Thermal Engineering*, 24(7), pp. 1009–1017. doi: 10.1016/j.applthermaleng.2003.11.014.

Coronas, A. (2020) 'Thermal Conversion Energy Technologies [subject code: 20755107]'. Tarragona: Universitat Rovira i Virgili.

Danfoss (2010) *Introduction to Hydronic Floor Heating*.

Deru, M. *et al.* (2011) 'U.S. Department of Energy commercial reference building models of the national building stock', *Publications (E),* (February 2011), pp. 1–118. Available at: http://digitalscholarship.unlv.edu/renew_pubs/44.

Districlima (2014) *About - Us*. Available at: http://www.districlima.com/en/about-us

(Accessed: 15 December 2020).

Districlima (2019) *Informative Documentation - Guía del usuario*. Available at: http://www.districlima.com/en/downloads (Accessed: 15 December 2020).

Districlima (2020) 'Guía Técnica del Cliente Acometidas, Subestaciones, y Circuitos', p. 98. Available at: http://www.districlima.com/districlima/uploads/descargas/guias-tecnicas/Guía Técnica Districlima 2020_rev0.pdf.

DOE (2017) *EnergyPlus, U.S. Department of Energy's*. Available at: https://energyplus.net/ (Accessed: 18 January 2021).

EnergyPlus (2016) *Weather Data – EnergyPlus, US Deparment of Energy*. Available at: https://energyplus.net/weather (Accessed: 15 November 2020).

Euroheat & Power (2008) 'Guidelines for District Heating Substations', *Euroheat & Power*, p. 68.

Euroheat & Power (2011) *District Heating in Buildings*. Brussels: Euroheat & Power.

Fantucci, S. *et al.* (2015) 'Thermal energy storage with super insulating materials: A parametrical analysis', *Energy Procedia*, 78, pp. 441–446. doi: 10.1016/j.egypro.2015.11.691.

Fritsche, U. R. and Greß, H.-W. (2015) 'Development of the Primary Energy Factor of Electricity Generation in the EU-28 from 2010-2013', *International Institute for Sustainability Analysis and Strategy (IINAS)*, (March). Available at: https://www.ehpa.org/fileadmin/red/03._Media/03.02_Studies_and_reports/2015_IINAS_PEF_EU-28_Electricity_2010-2013.pdf.

Harvey, L. D. D. (2020) 'Using modified multiple heating-degree-day (HDD) and cooling-degree-day (CDD) indices to estimate building heating and cooling loads', *Energy and Buildings*, 229, p. 110475. doi: 10.1016/j.enbuild.2020.110475.

Hellmann, H. M., Schweigler, C. and Ziegler, F. (1999) 'The characteristic equations of absorption chillers', in *International Sorption Heat Pump Conference*. Munich, Germany.

Herold, K. E., Radermacher, R. and Klein, S. A. (2016) *Absorption Chillers and Heat Pumps*. Second. CRC Press. doi: 10.1201/b19625.

Hüls Güido, W. *et al.* (2018) 'Performance of absorption chillers in field tests', *Applied Thermal Engineering*, 134(February), pp. 353–359. doi: 10.1016 /j.applthermaleng.

2018.02.013.

Hundy, G. F., Trott, A. R. and Welch, T. C. (2016) ‘The Refrigeration Cycle’, *Refrigeration, Air Conditioning and Heat Pumps*, pp. 19–39. doi: 10.1016/b978-0-08-100647-4.00002-4.

Hwang, R. L., Lin, T. P. and Kuo, N. J. (2006) ‘Field experiments on thermal comfort in campus classrooms in Taiwan’, *Energy and Buildings*, 38(1), pp. 53–62. doi: 10.1016/j.enbuild.2005.05.001.

Kozlov, A. *et al.* (2014) ‘Advanced Cooling Tower Concept for Commercial and Industrial’, in *ASME 2014 Power Conference*. Baltimore, Maryland, USA: ASME, pp. 1–7. Available at: https://asmedigitalcollection.asme.org/proceedings.

Kühn, A. (2013) *Thermally Driven Heat Pumps For Heating and Cooling*, *Heat Pumps in Chemical Process Industry*. TU Berlin. doi: 10.1201/9781315371030-8.

Kühn, A., Özgür-Popanda, C. and Ziegler, F. (2010) ‘A 10 kW indirectly fired absorption heat pump’, in *10th IEA Heat Pump Conference 2011*, pp. 1–12.

Li, Y. *et al.* (2011) ‘A new type of district heating system based on distributed absorption heat pumps’, *Energy*, 36(7), pp. 4570–4576. doi: 10.1016/j.energy.2011.03.019.

López-Ochoa, L. M. *et al.* (2020) ‘Energy renovation of residential buildings in cold mediterranean zones using optimized thermal envelope insulation thicknesses: The case of spain’, *Sustainability (Switzerland)*, 12(6). doi: 10.3390/su12062287.

López-Villada, J., Bruno, J. C. and Coronas, A. (2009) ‘Primary energy analysis of a solar cooling plant connected to a district heating and cooling network’, in *3rd International Conference on Solar Air Conditioning*. Palermo, Italy.

Lund, H. *et al.* (2010) ‘The role of district heating in future renewable energy systems’, *Energy*, 35(3), pp. 1381–1390. doi: 10.1016/j.energy.2009.11.023.

Martin, G. (2019) *District Heating Networks Design [Master Thesis]*. KTH School of Industrial and Engineering Management. Available at: https://www.diva-portal.org/smash/get/diva2:1372711/FULLTEXT01.pdf.

Martines Maradiaga, D. E. (2013) *Modelling and Data Validation for the Energy Analysis of Absorption Refrigeration Systems [Doctoral Thesis]*. Universitat Rovira i Virgili. Available at: https://www.tesisenred.net/bitstream/handle/10803/128508/PhD Thesis - David Martinez Maradiaga %28URV%29.pdf?sequence=1&isAllowed=y.

Martínez, P. J. and Pinazo, J. M. (2002) ‘A method for design analysis of absorption machines’, *International Journal of Refrigeration*, 25(5), pp. 634–639. doi: 10.1016/S0140-7007(01)00052-4.

Ministerio de Fomento (2015) ‘DA DB-HE / 1 (Documento de Apoyo al Documento Básico DB-HE Ahorro de energía)’, *Boletín Oficial del Estado*, pp. 1–19. Available at: https://www.codigotecnico.org/images/stories/pdf/ahorroEnergia/DA-DB-HE-1-Calculo_de_parametros_caracteristicos.pdf.

Mora, N. P. *et al.* (2017) ‘Solar district heating and cooling : A review’, *Energy Research*, (Agustus 2017), pp. 1–23. doi: 10.1002/er.3888.

Nasif, M. *et al.* (2010) ‘Membrane heat exchanger in HVAC energy recovery systems, systems energy analysis’, *Energy and Buildings*, 42(10), pp. 1833–1840. doi: 10.1016/j.enbuild.2010.05.020.

Noro, M. and Lazzarin, R. (2020) ‘PVT and ETC coupling for annual heating and cooling by absorption heat pumps’, *Sustainability (Switzerland)*, 12(17). doi: 10.3390/su12177042.

Petersen, S. *et al.* (2011) ‘Development of a 50 kW Absorption Chiller’, in *International Congress of Refrigeration*. Prague, Czech Republic, p. 8.

Petersen, S. *et al.* (2013) ‘New Absorption Chillers for CHCP or Solar Cooling System Technology’, in Kühn, A. (ed.) *Thermally driven heat pumps for heating and cooling*. Berlin: Universitätsverlag der TU Berlin, pp. 109–116. Available at: https://depositonce.tu-berlin.de/handle/11303/4023.

Phetteplace, G. *et al.* (2013) *District Heating Guide, ASHRAE*. Atlanta.

Prieto, J. (2020) ‘Modelling and Dynamic Simulation of Energy Conversion Systems [subject code: 207555202]’. Tarragona: Universitat Rovira i Virgili.

Sammeta, H. *et al.* (2011) ‘Effectiveness charts for counter flow corrugated plate heat exchanger’, *Simulation Modelling Practice and Theory*, 19(2), pp. 777–784. doi: 10.1016/j.simpat.2010.10.012.

Sayegh, M. A. *et al.* (2018) ‘Heat pump placement, connection and operational modes in European district heating’, *Energy and Buildings*, 166(February), pp. 122–144. doi: 10.1016/j.enbuild.2018.02.006.

Schneider, C. *et al.* (2013) ‘How will climate change modify river flow regimes in Europe?’, *Hydrology and Earth System Sciences*, 17(1), pp. 325–339. doi: 10.5194/hess-17-325-2013.

Skagestad, B. and Mildenstein, P. (2002) *District Heating and Connection Handbook*. Available at: https://www.districtheatingscotland.com/wp-content/uploads/2015/12/DistrictHeatingAndCoolingConnectionHandbook.pdf.

Sorknæs, P. *et al.* (2020) 'The benefits of 4th generation district heating in a 100% renewable energy system', *Energy*, 213, p. 119030. doi: 10.1016/j.energy.2020.119030.

Tafelmeier, S., Pernigotto, G. and Gasparella, A. (2017) 'Annual performance of sensible and total heat recovery in ventilation systems: Humidity control constraints for European climates', *Buildings*, 7(2), pp. 1–20. doi: 10.3390/buildings7020028.

Thorsen *et al.* (2018) 'Progression of District Heating – 1st to 4th generation', pp. 2019–2020. Available at: https://vbn.aau.dk/en/publications/progression-of-district-heating-1st-to-4th-generation-3.

TRNSYS16 (2007) 'TRNSYS16, a transient simulation program [SOFTWARE]'. Madison, Wis. : The Laboratory, 2007.

US Department of Energy (2012) *Existing Commercial Reference Buildings Constructed In or After 1980*. Available at: http://energy.gov/eere/buildings/existing-commercial-reference-buildings-constructed-or-after-1980 (Accessed: 1 December 2020).

Werner, S. (2013) *District Heating and Cooling, Reference Module in Earth Systems and Environmental Sciences*. Elsevier Inc. doi: 10.1016/b978-0-12-409548-9.01094-0.

Werner, S. (2017) 'International review of district heating and cooling', *Energy*, 137, pp. 617–631. doi: 10.1016/j.energy.2017.04.045.

Yu, F. W. *et al.* (2014) 'Review of standards for energy performance of chiller systems serving commercial buildings', *Energy Procedia*, 61, pp. 2778–2782. doi: 10.1016/j.egypro.2014.12.308.

Zecca, A. and Chiari, L. (2010) 'Fossil-fuel constraints on global warming', *Energy Policy*, 38(1), pp. 1–3. doi: 10.1016/j.enpol.2009.06.068.

Ziegler, F., Hellmann, H. M. and Schweigler, C. (1999) 'An approximative method for modelling the operating characteristics of advanced absorption chillers', in *20th International Congress of Refrigeration*. Sidney, Australia.

APPENDICES

Appendix 1: EES transcript for making TRNSYS external file of type107

```
"CHARACTERISTIC EQUATION FOR BEE - 50 kW"

"INPUT for External File - in Parametric Tables"
{f_DesignLoad=Fraction Design Load
t_Di_C=Desorber Inlet Temperature
t_Ai_C=Absorber Inlet Temperature
t_Eo_C=Evaporator Outlet Temperature}

COP_rated=0,823                          "nominal COP from Characteristic Equation"
Q_dot_E_rated=48,3 [kW]                  "nominal cooling capacity from Characteristic Equation"
Q_dot_D_rated=58,7 [kW]                  "nominal driving heat from Characteristic Equation"
Q_dot_AC_rated=Q_dot_E_rated+Q_dot_D_rated   "nominal rejected heat from Characteristic Equation"

t_Di=converttemp(C;K;t_Di_C)
t_Ai=converttemp(C;K;t_Ai_C)
t_Eo=converttemp(C;K;t_Eo_C)

K1=0,1: K2=-1: K3=-0,1
K4=1,1: K5=1,3: K6=0,1

KE_o=(1-(K1-K2)*K4/W_dot_E)^(-1)
K4|star=KE_o*K4
K5|star=KE_o*(K5-K6)+K6

W_dot_E=10 [kW/K]
W_dot_D=3,6 [kW/K]
W_dot_AC=113/(37-30) [kW/K]              "calculated from BINE 2012"

"Corresponding Characteristic Temperature Functions"
DELTADELTAt|star=t_Di*(1-K1)-t_Ai*(1-K2)+t_Eo*(1-K3)
DELTADELTAt|star_min=(t_Di-t_Ai)-DELTADELTAt|star


"Characteristic Equation for Heat Source and Driving Heat"
Q_dot_E=K4|star*DELTADELTAt|star
Q_dot_D=K5|star*DELTADELTAt|star + K6*DELTADELTAt|star_min
Q_dot_AC=Q_dot_E+Q_dot_D                 "with the global energy balance"


W_dot_E*(t_Ei-t_Eo)=Q_dot_E
W_dot_D*(t_Di-t_Do)=Q_dot_D
W_dot_AC*(t_Co-t_Ai)=Q_dot_AC

"Coversion to Celcius"
t_Ei_C=converttemp(K;C;t_Ei)
t_Do_C=converttemp(K;C;t_Do)
t_Co_C=converttemp(K;C;t_Co)

CoolingCapacity=(Q_dot_E/Q_dot_E_rated)*100
COP_R=Q_dot_E/Q_dot_D                    "COP for chiller"

"Output for External File"
f_DesignEnergyInput=(f_DesignLoad*(Q_dot_E_rated/Q_dot_E))*Q_dot_D*COP_rated/Q_dot_E_rated
f_capacity=Q_dot_E/Q_dot_E_rated
```

Appendix 2: TRNSYS External File of type107 – Performance data of BEE 50 kW in .dat file

```
0.00    0.10    0.20    0.30    0.40    0.50    0.60    0.70    0.80    0.90    1.00    !Fraction of Design Load
6       8       10      12      14      16                                              !Chilled Water Setpoint (CHW Set) [C]
20      25      30      35      40                                                      !Entering Cooling Water Temperature (ECWT) [C]
75      80      85      90                                                              !Inlet Hot Water Temperature (IHWT) [C]
0.8835  0       !f_Capacity and f_DesignEnergyInput at FDI=0 ;CHW_Set=6[C]; ECWT=20[C]; IHWT=75[C]
1       0       !f_Capacity and f_DesignEnergyInput at FDI=0 ;CHW_Set=6[C]; ECWT=20[C]; IHWT=80[C]
1.117   0       !f_Capacity and f_DesignEnergyInput at FDI=0 ;CHW_Set=6[C]; ECWT=20[C]; IHWT=85[C]
1.233   0       !f_Capacity and f_DesignEnergyInput at FDI=0 ;CHW_Set=6[C]; ECWT=20[C]; IHWT=90[C]
0.6244  0       !f_Capacity and f_DesignEnergyInput at FDI=0 ;CHW_Set=6[C]; ECWT=25[C]; IHWT=75[C]
0.741   0       !f_Capacity and f_DesignEnergyInput at FDI=0 ;CHW_Set=6[C]; ECWT=25[C]; IHWT=80[C]
0.8576  0       !f_Capacity and f_DesignEnergyInput at FDI=0 ;CHW_Set=6[C]; ECWT=25[C]; IHWT=85[C]
0.9742  0       !f_Capacity and f_DesignEnergyInput at FDI=0 ;CHW_Set=6[C]; ECWT=25[C]; IHWT=90[C]
0.3653  0       !f_Capacity and f_DesignEnergyInput at FDI=0 ;CHW_Set=6[C]; ECWT=30[C]; IHWT=75[C]
0.4819  0       !f_Capacity and f_DesignEnergyInput at FDI=0 ;CHW_Set=6[C]; ECWT=30[C]; IHWT=80[C]
0.5985  0       !f_Capacity and f_DesignEnergyInput at FDI=0 ;CHW_Set=6[C]; ECWT=30[C]; IHWT=85[C]
0.7151  0       !f_Capacity and f_DesignEnergyInput at FDI=0 ;CHW_Set=6[C]; ECWT=30[C]; IHWT=90[C
0.1062  0       !etc
0.2228  0
0.3394  0
0.456   0
0.1529  0
0.03627 0
0.08032 0
0.1969  0
0.9405  0
1.057   0
1.174   0
1.29    0
0.6814  0
0.798   0
0.9146  0
1.031   0
0.4223  0
0.5389  0
0.6555  0
0.7721  0
```

UNIVERSITAT
ROVIRA i VIRGILI